

Minimal dark matter: model and results

This article has been downloaded from IOPscience. Please scroll down to see the full text article.

2009 New J. Phys. 11 105005

(<http://iopscience.iop.org/1367-2630/11/10/105005>)

[The Table of Contents](#) and [more related content](#) is available

Download details:

IP Address: 132.166.160.145

The article was downloaded on 18/12/2009 at 13:46

Please note that [terms and conditions apply](#).

Minimal dark matter: model and results

Marco Cirelli^{1,3} and Alessandro Strumia²

¹ Institut de Physique Théorique, CNRS, URA 2306 and CEA/Saclay,
F-91191 Gif-sur-Yvette, France

² Dipartimento di Fisica dell'Università di Pisa and INFN, Italia
E-mail: marco.cirelli@cea.fr and Alessandro.Strumia@df.unipi.it

New Journal of Physics **11** (2009) 105005 (31pp)

Received 19 March 2009

Published 16 October 2009

Online at <http://www.njp.org/>

doi:10.1088/1367-2630/11/10/105005

Abstract. We recap the main features of minimal dark matter (MDM) and assess its status in the light of recent experimental data. The theory selects an electroweak 5-plet with hypercharge $Y = 0$ as a fully successful DM candidate, automatically stable against decay and with no free parameters: DM is a fermion with a 9.6 TeV mass. The direct detection cross-section, predicted to be 10^{-44} cm^2 , is within reach of next-generation experiments. DM is accompanied by a charged fermion 166 MeV heavier: we discuss how it might manifest. Thanks to an electroweak Sommerfeld enhancement of more than 2 orders of magnitude, DM annihilations into W^+W^- give, in the presence of a modest astrophysical boost factor, an e^+ flux compatible with the PAMELA excess (but not with the ATIC hint for a peak: MDM instead predicts a quasi-power-law spectrum), a \bar{p} flux concentrated at energies above 100 GeV, and photon fluxes comparable with present limits, depending on the DM density profile.

³ Author to whom any correspondence should be addressed.

Contents

1. Introduction	2
2. Construction of the MDM model	3
3. Cosmological relic density and mass determination	6
3.1. Mass splitting	9
4. Direct detection signatures	10
5. Indirect detection signatures	12
5.1. Positrons	13
5.2. Electrons + positrons	16
5.3. Antiprotons	18
5.4. Gamma rays	20
6. Collider searches	20
7. Other phenomenological signatures	21
7.1. Accumulator	21
7.2. Ultra high energy cosmic rays (UHECR)	22
8. Conclusions and outlook	23
Acknowledgments	26
Appendix A. Sommerfeld effects	26
Appendix B. Next-to-minimal MDM	27
References	29

1. Introduction

The quest for the identification of the missing mass of the universe has been with us for many decades now⁴. While explanations in terms of modifications of Newtonian gravity or general relativity become more and more contrived, evidence for the particle nature of such dark matter (DM) now comes from many astrophysical and cosmological observations. Non-baryonic new particles that may fulfil the role of DM have emerged in the latest decades within many Beyond the Standard Model (SM) theories, most notably supersymmetry (SUSY). These constructions try to naturally explain the hierarchy between the electroweak (EW) scale and the Planck scale and, in doing so, introduce a host of new particles with EW masses and interactions. Some of these particles can be good DM candidates (e.g. the lightest neutralino).

However, these approaches to the solution of the DM problem, while still the most popular, are beginning to face a sort of ‘impasse’. (i) The expected new physics at the EW scale has not appeared so far in collider experiments: the simplest solutions to the hierarchy problem are beginning to need uncomfortably high fine-tunings of their unknown parameters⁵. (ii) The presence of a number of unknown parameters (e.g. all particle masses) obscures the phenomenology of the DM candidates. (iii) The stability of the DM candidates is usually the result of extra features introduced by hand (e.g. R -parity in SUSY), most often also necessary to

⁴ Recent reviews include [1].

⁵ The fine-tuning argument was invented to motivate new physics at the weak scale. Its back-firing was addressed, after LEP2 negative searches, in [2].

recover many good properties of the SM that are lost in these extensions (automatic conservation of baryon number, lepton number, etc).

The minimal dark matter (MDM) proposal [3] pursues therefore a different and somewhat opposite direction: focusing on the DM problem only, we add to the SM the minimal amount of new physics (just one extra EW multiplet \mathcal{X}) and search for the minimal assignments of its quantum numbers (spin, isospin and hypercharge) that make it a good DM candidate without ruining the positive features of the SM. No *ad hoc* extra features are introduced: the stability of the successful candidates is guaranteed by the SM gauge symmetry and by renormalizability. Moreover, due to its minimality, the theory is remarkably predictive: no free parameters are present and therefore the phenomenological signatures can be univocally calculated, e.g. at colliders and for direct/indirect detection, up to the astrophysical and cosmological uncertainties.

The rest of the paper is organized as follows. In section 2, we review the theoretical aspects of the MDM model. We follow a constructive approach by scanning all the possible choices of quantum numbers and selecting the successful DM candidates: insisting on full minimality we will see that consistency and phenomenological constraints reject most of the candidates and actually individuate only one (the fermionic $SU(2)$ quintuplet with hypercharge $Y = 0$), of which we will study the phenomenology in the following sections. Note that since other candidates can be re-allowed by relaxing the request for full minimality (as we discuss in appendix B), the formulae and most of the phenomenological analysis are given in their most general form and can easily be adapted to these other candidates. In section 3, we present the computation of the cosmological relic density of MDM [4]: imposing the match with the measured density determines the DM mass. We also discuss the small mass splitting introduced by loop corrections. In section 4, we review the direct detection signatures of the candidate. In section 5, we focus on the indirect detection signatures, comparing the predictions [5] with recent data from satellite and balloon experiments: this promises to be the most interesting and stringent avenue of confrontation with data [6]. In section 6, we review what could be the signatures at colliders. Finally, in section 7 we discuss some other possible phenomenological features of the model. In appendix A, we briefly review the Sommerfeld enhancement of the annihilation cross section, discussed in more detail in [4, 5]. In appendix B, we list the options that open up for model building if the requirement of full minimality is relaxed. An executive summary of positive and negative features of the model, as well as an outlook towards the implications of future results, is given in section 8.

2. Construction of the MDM model

The MDM model is constructed by simply adding on top of the SM a single fermionic or scalar multiplet \mathcal{X} charged under the usual SM $SU_L(2) \times U_Y(1)$ EW interactions (that is: a WIMP; it is assumed not to be charged under $SU_C(3)$ strong interactions as the bounds are strong on this possibility⁶). Its conjugate $\bar{\mathcal{X}}$ belongs to the same representation, so that the theory is vector like

⁶ Strongly interacting, ‘hadronized’, DM is subject to a number of constraints analysed in [7] that leave only implausible windows open. Recently, Mack *et al* [7] went in the direction of closing those windows to safeguard Earth’s heat flow.

with respect to $SU_L(2)$ and anomaly free. The Lagrangian is ‘minimal’:

$$\mathcal{L} = \mathcal{L}_{\text{SM}} + \frac{1}{2} \begin{cases} \bar{\mathcal{X}}(i\not{D} + M)\mathcal{X}, & \text{for fermionic } \mathcal{X}, \\ |D_\mu \mathcal{X}|^2 - M^2|\mathcal{X}|^2, & \text{for scalar } \mathcal{X}. \end{cases} \quad (1)$$

The gauge-covariant derivative D_μ contains the known EW gauge couplings to the vectors bosons of the SM (Z , W^\pm and γ) and M is a tree-level mass term (the only free parameter of the theory). A host of additional terms (such as Yukawa couplings with SM fields) would in principle be present, but for successful candidates they will be forbidden by gauge and Lorentz invariance, as detailed below.

\mathcal{X} is fully determined by the assignments of its quantum numbers under the gauge group: the number of its $SU(2)_L$ components, $n = \{2, 3, 4, 5, \dots\}$ and the hypercharge Y . In table 1, we list all the potentially successful combinations, as we now proceed to discuss.

For a given assignment of n (first column of the table) there are a few choices of the hypercharge Y such that one component of the \mathcal{X} multiplet has electric charge $Q = T_3 + Y = 0$ (where T_3 is the usual ‘diagonal’ generator of $SU(2)_L$), as needed for a DM candidate. For instance, for the doublet $n = 2$, since $T_3 = \pm 1/2$, the only possibility is $Y = \mp 1/2$. For $n = 5$, one can have $Y = \{0, \pm 1, \pm 2\}$, and so on. We do not consider the case of the $n = 1$ singlet: lacking gauge interactions, even if it is ever produced in the early universe, it could not annihilate and remain with the correct relic amount by means of the standard freeze-out mechanism⁷.

The list of possible candidates has to stop at $n \leq 5(8)$ for fermions (scalars) because larger multiplets would accelerate the running of the $SU(2)_L$ coupling g_2 : demanding that the perturbativity of $\alpha_2^{-1}(E') = \alpha_2^{-1}(M) - (b_2/2\pi) \ln E'/M$ is maintained all the way up to $E' \sim M_{\text{Pl}}$ (since the Planck scale M_{Pl} is the cutoff scale of the theory) imposes the bound. In this formula, $b_2 = -19/6 + c g_\chi(n^2 - 1)/36$ with $c = 1$ for fermions, $c = 1/4$ for scalars and g_χ is the number of degrees of freedom in the multiplet.

In this list of candidates, those with $Y \neq 0$ have vector-like interactions with the Z boson that produce a tree-level spin-independent elastic cross sections

$$\sigma(\text{DM } \mathcal{N} \rightarrow \text{DM } \mathcal{N}) = c \frac{G_{\text{F}}^2 M_{\mathcal{N}}^2}{2\pi} Y^2 (N - (1 - 4s_{\text{W}}^2)Z)^2, \quad (2)$$

where $c = 1$ for fermionic DM and $c = 4$ for scalar DM [8]; Z and N are the number of protons and of neutrons in the target nucleus with mass $M_{\mathcal{N}}$ (we are assuming $M \gg M_{\mathcal{N}}$). This elastic cross section is 2–3 orders of magnitude above the present bounds [9, 10] from direct detection searches. Unless minimality is abandoned in an appropriate way (which we discuss in appendix B), such MDM candidates are therefore excluded and we will focus in the following on those with $Y = 0$.

Next, we need to inspect which of the remaining candidates are stable against decay into SM particles. The fourth column of table 1 shows some possible decay operators for each case. For instance, the fermionic 3-plet with hypercharge $Y = 0$ would couple through a Yukawa operator $\mathcal{X}LH$ with an SM lepton doublet L and a Higgs field H and decay in a very short time. This is not a viable DM candidate, unless the operator is eliminated by some ad hoc symmetries (see again appendix B). For another instance, the scalar 5-plet with $Y = 0$ would couple to four Higgs fields with a dimension 5 operator $\mathcal{X}HHH^*H^*/M_{\text{Pl}}$, suppressed by one power of the Planck scale. Despite the suppression, the resulting typical life-time $\tau \sim M_{\text{Pl}}^2 \text{TeV}^{-3}$ is shorter than the age of the universe, so that this is not a viable DM candidate.

⁷ We discuss the case of a scalar singlet with non-minimal additional interactions in appendix B.

Table 1. Book-keeping of the possible MDM candidates and selection of successful ones. Quantum numbers are listed in the first three columns. The fourth column indicates some decay modes into SM particles; modes listed in parenthesis correspond to dimension 5 operators. Candidates with $Y \neq 0$ are excluded by direct detection (DD) searches (unless appropriate non-minimalities are introduced, see appendix B), as indicated in the fifth column. Candidates with an open decay channel are excluded (unless some other non-minimalities are introduced, see appendix B), as indicated in the fifth column. Note that, for simplicity, the possibilities concerning the $SU_L(2)$ 6- and 8-plet are only sketched. Analogously, for the 7-plet we list the only interesting candidate. At the end of the game, the fully successful candidates are indicated by the shaded background: the fermionic 5-plet with $Y = 0$ and the scalar 7-plet with $Y = 0$. As for the latter non-minimal scalar quartic couplings are generically present (see appendix B), the former is overall preferred and we will refer to it as the MDM candidate in the paper.

Quantum numbers			DM can decay into	DD bound?	Stable?
$SU(2)_L$	$U(1)_Y$	Spin			
2	1/2	<i>S</i>	<i>EL</i>	×	×
2	1/2	<i>F</i>	<i>EH</i>	×	×
3	0	<i>S</i>	<i>HH*</i>	✓	×
3	0	<i>F</i>	<i>LH</i>	✓	×
3	1	<i>S</i>	<i>HH, LL</i>	×	×
3	1	<i>F</i>	<i>LH</i>	×	×
4	1/2	<i>S</i>	<i>HHH*</i>	×	×
4	1/2	<i>F</i>	<i>(LHH*)</i>	×	×
4	3/2	<i>S</i>	<i>HHH</i>	×	×
4	3/2	<i>F</i>	<i>(LHH)</i>	×	×
5	0	<i>S</i>	<i>(HHH*H*)</i>	✓	×
5	0	<i>F</i>	–	✓	✓
5	1	<i>S</i>	<i>(HH*H*H*)</i>	×	×
5	1	<i>F</i>	–	×	✓
5	2	<i>S</i>	<i>(H*H*H*H*)</i>	×	×
5	2	<i>F</i>	–	×	✓
6	1/2, 3/2, 5/2	<i>S</i>	–	×	✓
7	0	<i>S</i>	–	✓	✓
8	1/2, 3/2, ...	<i>S</i>	–	×	✓

Now, the crucial observation is that, given the known SM particle content, the large n multiplets cannot couple to SM fields and are therefore automatically stable DM candidates. This is the same reason why known massive stable particles (like the proton) are stable: decay modes consistent with renormalizability and gauge symmetry do not exist. In other words, for these candidates DM stability is explained by an ‘accidental symmetry’, like proton stability.

Among the candidates that survived all the previous constraints, only two possibilities then emerge: a $n = 5$ fermion, or a $n = 7$ scalar. But scalar states may have non-minimal quartic couplings with the Higgs field (see appendix B). We will then set the 7-plet aside and focus on the fermionic 5-plet for minimality in the following.

In summary, the ‘MDM’ construction singles out a

$$\text{fermionic } SU(2)_L \text{ 5-plet with hypercharge } Y = 0$$

as providing a fully viable, automatically stable DM particle. It is called ‘MDM’ since it is described by the minimal gauge-covariant Lagrangian that one obtains adding the minimal amount of new physics to the SM in order to explain the DM problem.

3. Cosmological relic density and mass determination

Assuming that DM arises as a thermal relic in the early Universe, via the standard freeze-out process, we can compute the abundance of MDM as a function of its mass M . In turn, requiring that MDM makes all the observed DM measured by cosmology, $\Omega_{\text{DM}} h^2 = 0.110 \pm 0.005$,⁸ we can univocally determine M . As a general rule of thumb, it is well known (see footnote 4) that $\Omega_{\text{DM}} h^2 \approx 3 \times 10^{-27} \text{ cm}^3 \text{ s}^{-1} / \langle \sigma_A \beta \rangle$ and that a particle with weak couplings α_w has a $\langle \sigma_A \beta \rangle \approx \alpha_w^2 M_{\text{DM}}^{-2}$ that matches Ω_{DM} for a typical weak scale mass (the so-called WIMP miracle). This is therefore what is to be expected for a pure WIMP model such as MDM.

More precisely, the computation of the relic abundance has to be performed by solving the relevant Boltzmann equation (as we review below) in terms of the detailed annihilation cross section of two MDM particles into any SM state. We include the dominant s-wave contribution, but also the subdominant p-wave, which yields an $\mathcal{O}(5\%)$ correction on the final Ω_{DM} and the effect of the renormalization of the SM gauge couplings up to the MDM mass scale M (also an $\mathcal{O}(5\%)$ modification). On top of this standard computation, however, we have to include the non-perturbative EW Sommerfeld corrections, that have a very relevant effect. In fact, this phenomenon significantly enhances non-relativistic annihilations of DM particles with mass $M \gtrsim M_V/\alpha$, when they exchange force mediators of mass M_V with a coupling strength α . In the case of MDM, this is simply the ordinary SM weak force mediated by W^\pm and Z , and we will verify *a posteriori* that the relation $M \gtrsim M_{W^\pm}/\alpha_2$ is indeed verified for the MDM masses M that we will obtain. Therefore the Sommerfeld effect is automatically present in the theory and has to be taken into account. We review the basics of the Sommerfeld effect in appendix A.

Let us now describe in more detail the machinery of the computation and the results in our specific case. The generic Boltzmann equation that governs the DM abundance as a function of the temperature T reads

$$sZH_z \frac{dY}{dz} = -2 \left(\frac{Y^2}{Y_{\text{eq}}^2} - 1 \right) \gamma_A, \quad \gamma_A = \frac{T}{64\pi^4} \int_{4M^2}^{\infty} ds s^{1/2} K_1 \left(\frac{\sqrt{s}}{T} \right) \hat{\sigma}_A(s), \quad (3)$$

where $z = M/T$, K_1 is a Bessel function, $Z = (1 - \frac{1}{3} \frac{z}{g_s} \frac{dg_s}{dz})^{-1}$, the entropy density of SM particles is $s = 2\pi^2 g_{*s} T^3/45$, $Y = n_{\text{DM}} s^{-1}$ where n_{DM} is the number density of DM particles

⁸ These numbers summarize various recent global analyses of cosmological data within the Λ CDM model that found compatible values and uncertainties [11].

plus antiparticles, and Y_{eq} is the value that Y would have in thermal equilibrium. The adimensional ‘reduced annihilation cross section’ is defined as

$$\hat{\sigma}_A(s) = \int_{-s}^0 dt \sum \frac{|\mathcal{A}|^2}{8\pi s}, \quad (4)$$

where s and t are the Madelstam variables and the sum runs over all DM components and over all the annihilation channels into all SM vectors, fermions and scalars, assuming that SM masses are negligibly small. In the case of MDM, we can write a single equation for the total DM density, in particular, neglecting the small splitting ΔM that we will discuss in section 3.1, because DM scattering with SM particles maintain thermal equilibrium within and between the single components. In this way, the formula automatically takes into account all co-annihilations among the multiplet components. We also ignore the Bose–Einstein and Fermi–Dirac factors as they are negligible at the temperature $T \sim M/26$ relevant for DM freeze-out.

In full generality, for fermionic DM with $SU(2)_L \times U(1)_Y$ quantum numbers n and Y we get

$$\hat{\sigma}_A = \frac{g_\chi}{24\pi n} \left[(9C_2 - 21C_1)\beta + (11C_1 - 5C_2)\beta^3 - 3(2C_1(\beta^2 - 2) + C_2(\beta^2 - 1)^2) \ln \frac{1+\beta}{1-\beta} \right] + g_\chi \left(\frac{3g_2^4(n^2 - 1) + 20g_Y^4 Y^2}{16\pi} + \frac{g_2^4(n^2 - 1) + 4g_Y^4 Y^2}{128\pi} \right) \left(\beta - \frac{\beta^3}{3} \right), \quad (5)$$

while for scalar DM we get

$$\hat{\sigma}_A = \frac{g_\chi}{24\pi n} \left[(15C_1 - 3C_2)\beta + (5C_2 - 11C_1)\beta^3 + 3(\beta^2 - 1)(2C_1 + C_2(\beta^2 - 1)) \ln \frac{1+\beta}{1-\beta} \right] + g_\chi \left(\frac{3g_2^4(n^2 - 1) + 20g_Y^4 Y^2}{48\pi} + \frac{g_2^4(n^2 - 1) + 4g_Y^4 Y^2}{384\pi} \right) \cdot \beta^3, \quad (6)$$

where $x = s/M^2$ and $\beta = \sqrt{1 - 4/x}$ is defined in the DM DM center-of-mass frame. The first line gives the contribution of annihilation into vectors, the second line contains the sum of the contributions of annihilations into SM fermions and vectors, respectively. The gauge group factors are defined as

$$C_1 = \sum_{A,B} \text{Tr} T^A T^A T^B T^B = g_Y^4 n Y^4 + g_2^2 g_Y^2 Y^2 \frac{n(n^2 - 1)}{2} + g_2^4 \frac{n(n^2 - 1)^2}{16}, \quad (7)$$

$$C_2 = \sum_{A,B} \text{Tr} T^A T^B T^A T^B = g_Y^4 n Y^4 + g_2^2 g_Y^2 Y^2 \frac{n(n^2 - 1)}{2} + g_2^4 \frac{n(n^2 - 1)(n^2 - 5)}{16}, \quad (8)$$

where the sum is over all SM vectors $A = \{Y, W^1, W^2, W^3\}$ with gauge coupling generators T^A . We have defined g_χ as the number of DM degrees of freedom for a multiplet with $Y = 0$: $g_\chi = n$ for scalar DM, $g_\chi = 2n$ ($4n$) for fermionic Majorana (Dirac) DM.

The DM freeze-out abundance is accurately determined by the leading two terms of the expansion for small β that describe the s-wave and the p-wave contributions. This approximation allows us to analytically do the thermal average in equation (3):

$$\hat{\sigma}_A \stackrel{\beta \rightarrow 0}{\simeq} c_s \beta + c_p \beta^3 + \dots \quad \text{implies} \quad \gamma_A \stackrel{\beta \rightarrow 0}{\simeq} \frac{MT^3 e^{-2M/T}}{32\pi^3} \left[c_s + \frac{3T}{2M} \left(c_p + \frac{c_s}{2} \right) + \dots \right]. \quad (9)$$

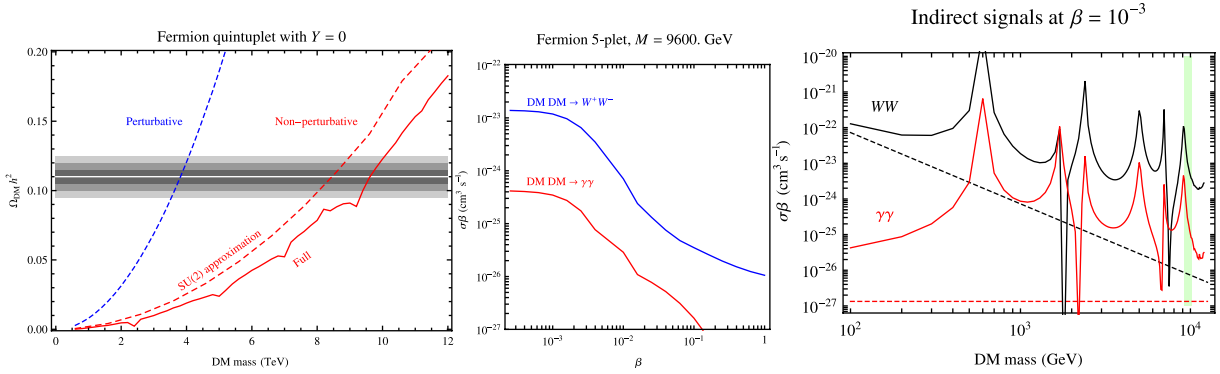


Figure 1. Left panel: the relic abundance of the MDM 5-plet as a function of its mass M . The solid red line corresponds to the full result that includes non-perturbative Sommerfeld-enhanced annihilations (the dashed red line corresponds to the computation in the $SU(2)_L$ -symmetric limit), whereas the dashed blue includes perturbative s-wave and p-wave tree-level annihilations. The horizontal band corresponds to the measured $\Omega_{\text{DM}}h^2$, so that its intersection with the red line individuates the DM mass (slightly below 10 TeV) and indicates its uncertainty interval. Central panel: velocity dependence of the Sommerfeld-enhanced MDM annihilation cross section. Right panel: the DM DM annihilation cross section in the galactic halo today, relevant for indirect detection signatures discussed in section 5. The dashed lines show what the perturbative result would be without Sommerfeld corrections.

This general formalism can now be easily reduced to the case of the MDM particle, the fermionic 5-plet with $Y = 0$. The s-wave and p-wave coefficients are simply given by

$$c_s = \frac{1035}{8\pi} g_2^4, \quad c_p = \frac{1215}{8\pi} g_2^4. \quad (10)$$

The large figures at the numerators simply reflect the ‘large’ number ($n = 5$) of components in the multiplet: their coannihilations make for an overall large cross-section parameter.

As anticipated, on top of this the annihilation cross sections are enhanced by the non-perturbative Sommerfeld effect. The effect is strongly dependent on the velocity β (in units of c) of the DM particles: the total annihilation cross section $\sigma\beta$ grows as $\beta \rightarrow 0$ as illustrated in figure 1(b). MDM annihilations at the epoch of freeze-out (when $\beta \sim 0.2$) are enhanced by a factor of a few; astrophysical signals due to MDM annihilations in the galaxy today (where $\beta \sim 10^{-3}$) will be much more enhanced, up to a few orders of magnitude, as discussed in section 5.

Solving the Boltzmann equation with all these ingredients allows us to compute the relic abundance of the MDM particle $\Omega_{\text{DM}} = Y(z \rightarrow \infty) s M / \rho_{\text{crit}}$ as a function of its mass M . The numerical result is plotted in figure 1(a). For a given value of the mass, the impact of non-perturbative corrections is relevant, as they enhance the annihilation cross section and therefore reduce the corresponding relic abundance. Matching the relic abundance to the measured $\Omega_{\text{DM}}h^2 = 0.110 \pm 0.005$ allows us therefore to determine

$$M = (9.6 \pm 0.2) \text{ TeV}. \quad (11)$$

For comparison, the value without Sommerfeld corrections (blue dashed curve in figure 1(a)) would be about 4 TeV.

In summary: the only free parameter of the theory, the DM mass M , is fixed by matching the observed relic DM abundance. Not surprisingly, its value turns out to be broadly in the TeV range, because MDM is a pure WIMP model for which the so-called ‘WIMP miracle’ applies. The value actually ends up being somewhat higher (equation (11)) because the 5-plet has many components so that coannihilations are important *and* because Sommerfeld corrections enhance the annihilation cross section.

3.1. Mass splitting

Supersymmetric models typically feature a model-dependent EW-scale mass difference between the neutralino DM candidate and its chargino partners: the (typically multi-GeV) mass difference originates through tree-level mass mixing. In the MDM case, instead, at tree level all the components of the multiplet have the same mass M computed in the previous section, and then one-loop EW corrections make the charged components slightly heavier than the neutral one (if the opposite were true, one would have a charged lightest stable particle, which is of course not phenomenologically allowed).

In full generality, for a fermionic or scalar candidate with overall mass M and hypercharge Y , the mass difference induced by loops of SM gauge bosons between two components of \mathcal{X} with electric charges Q and Q' is found to be

$$M_Q - M_{Q'} = \frac{\alpha_2 M}{4\pi} \left\{ (Q^2 - Q'^2) s_w^2 f\left(\frac{M_Z}{M}\right) + (Q - Q')(Q + Q' - 2Y) \right. \\ \left. \times \left[f\left(\frac{M_W}{M}\right) - f\left(\frac{M_Z}{M}\right) \right] \right\}, \quad (12)$$

where

$$f(r) = \begin{cases} +r [2r^3 \ln r - 2r + (r^2 - 4)^{1/2}(r^2 + 2) \ln A] / 2, & \text{for a fermion,} \\ -r [2r^3 \ln r - kr + (r^2 - 4)^{3/2} \ln A] / 4, & \text{for a scalar,} \end{cases} \quad (13)$$

with $A = (r^2 - 2 - r\sqrt{r^2 - 4})/2$ and s_w the sine of the weak angle. In the numerically relevant limit $M \gg M_{W,Z}$ the one-loop corrections get the universal value $f(r) \xrightarrow{r \rightarrow 0} 2\pi r$. For the fermionic 5-plet with $Y = 0$, the splitting between the neutral component (the DM particle) and its $Q = \pm 1$ partners equals therefore to

$$\Delta M = \alpha_2 M_W \sin^2 \frac{\theta_W}{2} = (166 \pm 1) \text{ MeV}. \quad (14)$$

In general, the mass splitting between charged and neutral components can be intuitively understood in terms of the *classical* non-Abelian Coulomb energy (the energy stored in the EW electric fields that a point-like charge at rest generates around itself, which can be thought as an additional contribution to its mass with respect to the mass of an equivalent neutral particle). Indeed, for a scalar or fermion with a gauge coupling g under a vector with mass M_V , the Coulomb energy is:

$$\delta M = \int d^3r \left[\frac{1}{2} (\vec{\nabla} \varphi)^2 + \frac{M_V}{2} \varphi^2 \right] = \frac{\alpha}{2} M_V + \infty, \quad \varphi(r) = \frac{g e^{-M_V r / \hbar}}{4\pi r}.$$

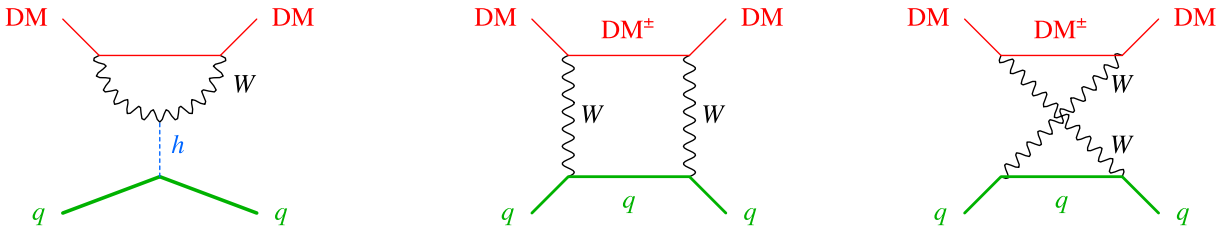


Figure 2. One-loop DM/quark scattering for fermionic MDM with $Y = 0$ (two extra graphs involving the four particle vertex exist in the case of scalar MDM).

As $SU(2)_L$ invariance is restored at distances $r \ll 1/M_{W,Z}$, the UV divergent term cancels out when computing the correction to the intra-multiplet mass splitting. Therefore we understand why the effect in the limit $M \gg M_{W,Z}$ does not depend on the DM spin, and why the neutral component is lighter than the charged ones. This intuitive picture allows us to guess that, when considering the low-energy DM/nuclei relevant for DM DD, the spin-independent cross section will be suppressed only by $1/M_{W,Z}^2$ (and not by the much smaller $1/M^2$), because what scatters is the cloud of EW electric fields that extend up to $r \sim 1/M_{W,Z}$. This agrees with the Feynman diagram computation presented in the next section.

4. Direct detection signatures

Direct searches for DM aim to detect the recoils of nuclei in a low background detector produced by the rare collisions of DM halo particles on such nuclei. So far, the DAMA/Libra experiment [13] has reported the detection of an annual modulation of the total number of events compatible with the effect that the motion of the Earth in the DM halo would produce. The CDMS [9] and xenon [10] experiments have published exclusion bounds.

As discussed in section 2, MDM candidates with $Y = 0$ have vanishing $\text{DM}\mathcal{N}$ direct detection cross sections at tree level (see equation (17)). The scattering on nuclei \mathcal{N} proceeds therefore at one loop, via the diagrams in figure 2 that involve one of the charged components \mathcal{X}^\pm of the multiplets. An explicit computation of these one-loop diagrams is needed to understand qualitatively and quantitatively the resulting cross section. Non-relativistic MDM/quark interactions of fermionic \mathcal{X} with mass $M \gg M_W \gg m_q$ are described by the effective on-shell Lagrangian

$$\mathcal{L}_{\text{eff}}^W = (n^2 - (1 \pm 2Y)^2) \frac{\pi \alpha_2^2}{16M_W} \sum_q \left[\left(\frac{1}{M_W^2} + \frac{1}{m_h^2} \right) [\bar{\mathcal{X}}\mathcal{X}]m_q[\bar{q}q] - \frac{2}{3M} [\bar{\mathcal{X}}\gamma_\mu\gamma_5\mathcal{X}][\bar{q}\gamma_\mu\gamma_5q] \right], \quad (15)$$

where the + (−) sign holds for down-type (up-type) quarks $q = \{u, d, s, c, b, t\}$, m_h is the Higgs mass and m_q are the quark masses. The first operator gives dominant spin-independent effects and is not suppressed by M ; the second operator is suppressed by one power of M and gives spin-dependent effects. Parameterizing the nucleonic matrix element as

$$\langle N | \sum_q m_q \bar{q}q | N \rangle \equiv f m_N, \quad (16)$$

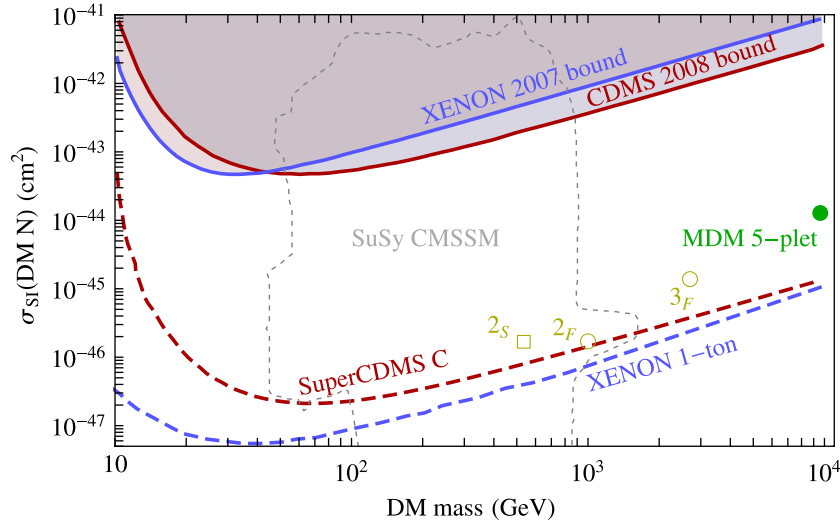


Figure 3. Parameter space of the spin-independent cross section per nucleon. The MDM 5-plet is represented by the green dot. The prediction is univocal (having assumed that the matrix element $f = 1/3$ and 115 GeV as a value for the Higgs mass), whereas typical minimal SUSY models span a large portion of the parameter space, suggested here by the area with dotted contours. The dashed lines indicate the sensitivity of some future experiments⁹. Other non-minimal candidates, discussed in appendix B, are reported for completeness: the fermionic 3-plet and the fermion and scalar doublet.

where m_N is the nucleon mass, the spin-independent DM cross section on a target nucleus \mathcal{N} with mass $M_{\mathcal{N}}$ is given by

$$\sigma_{\text{SI}}(\text{DM } \mathcal{N} \rightarrow \text{DM } \mathcal{N}) = (n^2 - 1)^2 \frac{\pi \alpha_2^4 M_{\mathcal{N}}^4 f^2}{64 M_W^2} \left(\frac{1}{M_W^2} + \frac{1}{m_h^2} \right)^2. \quad (17)$$

The case of scalar \mathcal{X} is not much different: the M -independent contribution to σ_{SI} is equal to the fermionic result of equation (17) but there is no spin-dependent effect.

Assuming $m_h = 115$ GeV and $f \approx 1/3$ (QCD uncertainties induce a one order-of-magnitude indetermination on σ_{SI})¹⁰ we find therefore for the fermionic MDM 5-plet

$$\sigma_{\text{SI}} = 1.2 \times 10^{-44} \text{ cm}^2. \quad (18)$$

As usual [1, 14, 15], σ_{SI} is defined to be the cross section per nucleon. The prediction is a definite number (as opposed to the large areas in the plane M/σ that is covered by typical supersymmetric constructions by varying the model parameters) and figure 3 shows that this value is within or very close to the sensitivities of experiments currently under study, such as Super-CDMS and xenon 1-ton (see footnote 10). The annual modulation effect of the DAMA/Libra experiment [13] cannot be explained by MDM candidates, since they have too

⁹ More precisely, one needs to consider the effective Lagrangian for off-shell quarks, finding various operators that become equivalent only on-shell. Their nucleon matrix elements can differ; we ignore this issue because presently it is within the QCD errors.

¹⁰ For the XENON project and for the SuperCDMS project see [16]. Useful comparisons can be done using the tools in dendera.berkeley.edu/plotter/entryform.html.

large masses and too small cross sections with respect to the properties of a WIMP compatible with the effect.

5. Indirect detection signatures

Indirect searches are one of the most promising ways to detect DM. DM particles in the galactic halo are expected to annihilate and produce fluxes of cosmic rays that propagate through the galaxy and reach the Earth. Their energy spectra carry important information on the nature of the DM particle (mass and primary annihilation channels). Many experiments are searching for signatures of DM annihilations in the fluxes of γ rays, positrons and antiprotons and there has been recently a flurry of experimental results in this respect:

- data from the PAMELA satellite show a steep increase in the energy spectrum of the positron fraction $e^+/(e^+ + e^-)$ above 10 GeV up to 100 GeV [17], compatibly with previous less certain hints from HEAT [18] and AMS-01 [19];
- data from the PAMELA also show no excess in the \bar{p}/p energy spectrum [20] compared with the predicted background;
- the balloon experiments ATIC-2 [21] and PPB-BETS [22] report the presence of a peak in the $e^+ + e^-$ energy spectrum at around 500–800 GeV;
- the HESS telescope has also reported the measurement [23] of the $e^+ + e^-$ energy spectrum above energies of 600 GeV up to a few TeV: the data points show a steepening of the spectrum, which is compatible both with the ATIC peak (which cannot, however, be fully tested) and with a power law with index -3.05 ± 0.02 and a cutoff at ≈ 2 TeV.

Some words of caution apply to the balloon results: the Monte Carlo simulations that such experiments need in order to tag e^\pm and infer their energy have been tested only up to LEP energies; the excess is based on just a few data-points that are not cleanly consistent between ATIC-2 and the smaller PPB-BETS; emulsion chambers (EC) balloon experiments [25] do not show evidence for an excess, although they have larger uncertainties. The upcoming results of the FERMI/LAT mission on the $e^+ + e^-$ energy spectrum [26] will hopefully soon indicate in a more definitive and precise way the shape of the spectrum.

In full generality [27], the PAMELA positron and antiproton data, if interpreted in terms of DM, indicate either: (i) a DM particle of any mass (above about 100 GeV) that annihilates only into leptons, not producing therefore unseen antiprotons or (ii) a DM particle with a mass around or above 10 TeV, that can annihilate into any channel. Adding the balloon data, the mass is pinned down to about 1 TeV and only leptonic channels are allowed.

Minimal DM has definite predictions for the fluxes of positrons, antiprotons and gamma rays, presented in [5] before the announcements of the experimental results (and even before some of the relevant experiments, such as FERMI, started taking data). The comparison with the data that are now available allows us to fix the astrophysical uncertainties and test the model. The MDM 5-plet annihilates at tree level into W^+W^- , and at loop level into $\gamma\gamma$, γZ , ZZ . The relative cross sections are significantly affected by the non-perturbative Sommerfeld corrections discussed in section 3 and in appendix A. The best-fit values are:

$$\langle\sigma v\rangle_{WW} = 1.1 \times 10^{-23} \text{cm}^3 \text{s}^{-1}, \quad \langle\sigma v\rangle_{\gamma\gamma} = 3 \times 10^{-25} \text{cm}^3 \text{s}^{-1}. \quad (19)$$

Annihilation cross sections into γZ and ZZ are given by

$$\sigma_{\gamma Z} = 2\sigma_{\gamma\gamma} / \tan^2 \theta_W = 6.5\sigma_{\gamma\gamma}, \quad \sigma_{ZZ} = \sigma_{\gamma\gamma} / \tan^4 \theta_W = 10.8\sigma_{\gamma\gamma} \quad (20)$$

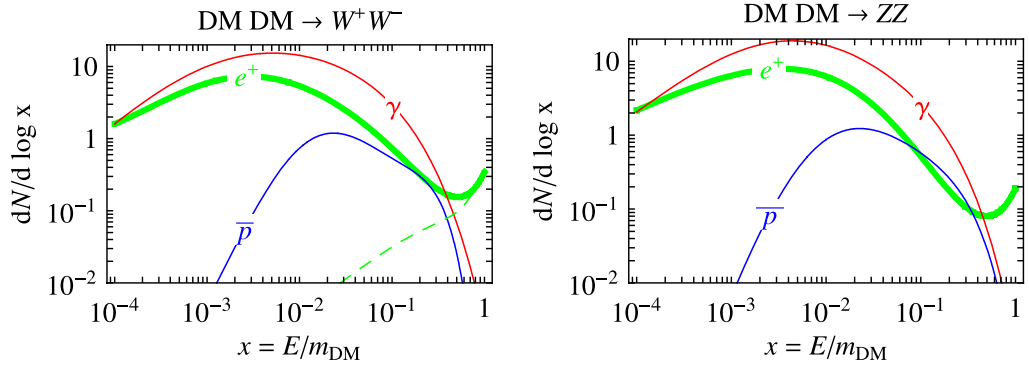


Figure 4. Energy spectra of e^+ , \bar{p} , γ produced by non-relativistic DM DM annihilations into W^+W^- and into ZZ , the only two relevant channels for MDM (together with $\gamma\gamma$, which produces a γ line at the MDM mass, and γZ , which can be deduced from the $\gamma\gamma$ and ZZ channels). The e^+ have a secondary component (dashed green line shown on the W^+W^- plot), that dominates at large $x \sim 1$.

(that actually hold for any MDM candidate with $Y = 0$). However, as shown in figure 1(c), as a consequence of Sommerfeld corrections the DM DM annihilation cross sections exhibit a quite steep dependence on M_{DM} and can vary by about one order of magnitude around these central values within the range allowed at 3σ by the cosmological DM abundance. The cross section also depends on the DM velocity v , reaching a maximal value for $v \rightarrow 0$, as shown in figure 1(b). The average DM velocity in our galaxy, $v \approx 10^{-3}$, is however low enough that σv is close to its maximal value, which we assume.

The energy spectra of e^+ , \bar{p} and γ per annihilation at production, as generated by PYTHIA supplemented by appropriate custom routines that allow us to take into account the spin correlations of SM vectors¹¹, are represented in figure 4. We next need to consider where these fluxes of particles are produced in the galaxy and how they propagate to the Earth.

5.1. Positrons

The positron flux per unit energy from DM annihilations in any point in space and time is given by $\Phi_{e^+}(t, \vec{x}, E) = v_{e^+} f / 4\pi$ (units $1 \text{ GeV}^{-1} \text{ cm}^{-2} \text{ s}^{-1} \text{ sr}^{-1}$) where v_{e^+} is the positron velocity (essentially equal to c in our regimes of interest) and the positron number density per unit energy, $f(t, \vec{x}, E) = dN_{e^+}/dE$, obeys the diffusion-loss equation

$$\frac{\partial f}{\partial t} - K(E) \cdot \nabla^2 f - \frac{\partial}{\partial E} (b(E)f) = Q \quad (21)$$

with diffusion coefficient $K(E) = K_0(E/\text{GeV})^\delta$ and energy loss coefficient $b(E) = E^2/(\text{GeV} \cdot \tau_E)$ with $\tau_E = 10^{16} \text{ s}$. They respectively describe transport through the turbulent magnetic fields and energy loss due to synchrotron radiation and inverse Compton scattering on CMB photons and on infrared galactic starlight. Equation (21) is solved in a diffusive region with the shape of a solid flat cylinder that sandwiches the galactic plane, with height $2L$ in the

¹¹ More details are given in [5].

Table 2. Propagation parameters for charged (anti)particles in the galaxy (from [29] and [35]).

Model	Positrons		Antiprotons			
	δ	K_0 (kpc ² Myr ⁻¹)	δ	K_0 (kpc ² Myr ⁻¹)	V_{conv} (km s ⁻¹)	L (kpc)
MIN	0.85	0.0016	0.55	0.00595	13.5	1
MED	0.70	0.0112	0.70	0.0112	12	4
MAX	0.46	0.0765	0.46	0.0765	5	15

z -direction and radius $R = 20$ kpc in the r -direction¹². The location of the solar system corresponds to $\vec{x} = (r_\odot, z_\odot) = (8.5 \text{ kpc}, 0)$. The boundary conditions impose that the positron density f vanishes on the surface of the cylinder, outside of which positrons freely propagate and escape. Values of the propagation parameters δ , K_0 and L are deduced from a variety of cosmic ray data and modelizations. They represent a source of uncertainty over which to scan in order to reach the final predictions for the fluxes. We consider the sets presented in table 2 [29]. Finally, the source term due to DM DM annihilations in each point of the halo with DM density $\rho(\vec{x})$ is

$$Q = \frac{1}{2} \left(\frac{\rho}{M_{\text{DM}}} \right)^2 f_{\text{inj}}, \quad f_{\text{inj}} = \sum_k \langle \sigma v \rangle_k \frac{dN_{e^+}^k}{dE}, \quad (22)$$

where k runs over all the channels with positrons in the final state, with the respective thermal averaged cross sections σv . Several galactic DM profiles are computed on the basis of numerical simulations: isothermal [31], Einasto [32], Navarro–Frenk–White [33] and Moore [34] (roughly in order of cusiness at the galactic center). The choice of profile introduces a further element of astrophysical uncertainty over which to scan.

The solution for the positron flux at Earth can be written in a useful semi-analytical form [29, 30]:

$$\Phi_{e^+}(E, \vec{r}_\odot) = B \frac{v_{e^+}}{4\pi b(E)} \frac{1}{2} \left(\frac{\rho_\odot}{M_{\text{DM}}} \right)^2 \int_E^{M_{\text{DM}}} dE' f_{\text{inj}}(E') \cdot I(\lambda_{\text{D}}(E, E')), \quad (23)$$

where $B \geq 1$ is an overall boost factor discussed below, $\lambda_{\text{D}}(E, E')$ is the diffusion length from energy E' to energy E . The adimensional ‘halo function’ $I(\lambda_{\text{D}})$ [29] fully encodes the galactic astrophysics and is independent on the particle physics model. Its possible shapes are plotted in figure 5(a) for most common choices of DM density profiles and set of positron propagation parameters.

The flux of positrons from DM annihilations has to be summed to the expected astrophysical background. We take the latter from the CR simulations of [36] as parameterized in [37] by $\Phi_{e^+}^{\text{bkg}} = 4.5 E^{0.7} / (1 + 650 E^{2.3} + 1500 E^{4.2})$ for positron and $\Phi_{e^-}^{\text{bkg}} = \Phi_{e^-}^{\text{bkg, prim}} + \Phi_{e^-}^{\text{bkg, sec}} = 0.16 E^{-1.1} / (1 + 11 E^{0.9} + 3.2 E^{2.15}) + 0.70 E^{0.7} / (1 + 110 E^{1.5} + 580 E^{4.2})$ for electrons, with E always in units of GeV. These not-so-recent background computations have recently been revised and questioned [38]: background shapes with a downturn around energies of a few GeV have been investigated in order to incorporate the PAMELA excess as a feature of the background.

¹² The new standard ‘two-zone diffusion model’ introduced in [28].

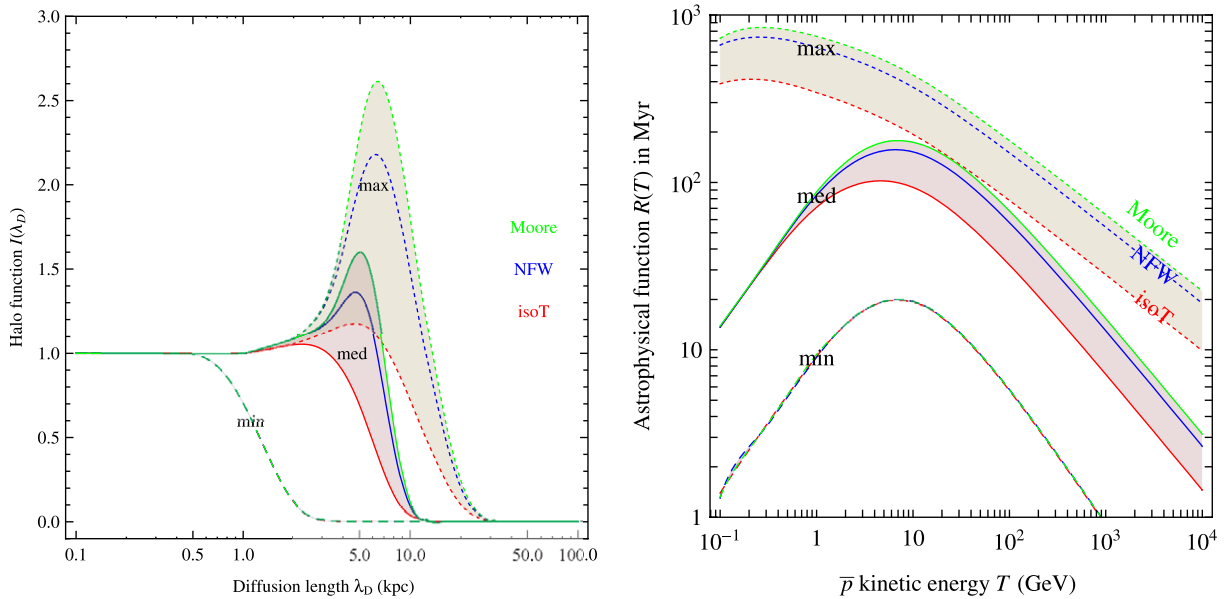


Figure 5. The astrophysical propagation functions for positrons and antiprotons. Left: the ‘halo function’ $I(\lambda_D)$ of equation (23) that encodes the astrophysics of DM DM annihilations into positrons and their propagation up to the earth. The diffusion length is related to energy losses as in equation (14) of [5], that also provides fit functions for all cases. Right: the somewhat analogous \bar{p} astrophysical function $R(T)$ of equation (25). In both cases, the dashed (solid) [dotted] bands assumes the min (med) [max] propagation configuration of table 2. Each band contains three lines that correspond to the isothermal (red lower lines), NFW (blue middle lines) and Moore (green upper lines) DM density profiles.

Finally, the DM density in our galaxy might have local clumps that would enhance the positron flux by an unknown ‘boost factor’ $B \geq 1$. We take it as energy independent: this is a simplifying (but widely used) assumption. Detailed recent studies [39]–[42] find that a certain energy dependence can be present, subject to the precise choices of the astrophysical parameters. Within the uncertainty, these studies also converge towards small values of B (except for extreme scenarios), with $B = \mathcal{O}(10)$ still allowed.

On the basis of the ingredients above, the fluxes at Earth of positrons from MDM annihilations can be compared with the experimental results. This is shown in figure 6. One sees that the predictions agree very well with the PAMELA results on the whole range of energies. We have assumed $B = 50$, which is the value found to provide the best fit to positrons, electrons and antiprotons data (discussed below) combined. This is quite a large value, in tension with the determinations discussed above. On the other hand, lower values (down to about 20) would still give a reasonably good fit and in any case the MDM annihilation cross sections of equation (19) carry a one order-of-magnitude uncertainty. In order to be conservative, we prefer to quote the boost value ‘as is’, instead of looking for possible optimizations. The figure also illustrates that the DM signal is only very mildly affected by changing the DM density profile (dotted lines). It somewhat depends on the e^+ propagation model in our galaxy (dashed lines); this

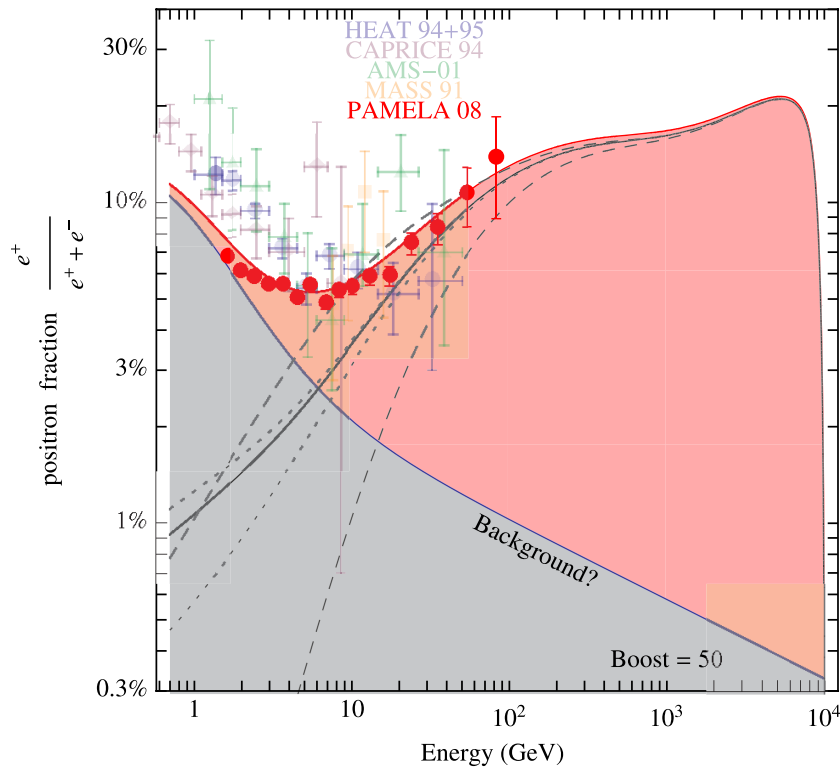


Figure 6. Positron fraction. The positron fraction from MDM galactic annihilations is compared with the data from PAMELA and previous experiments. We have taken a boost factor of 50 (see text). We show the DM signal (the lines) and the total positron fraction when summed to the background (shaded area). The main result (solid line and shaded area) is computed assuming a benchmark NFW DM profile and MED propagation parameters. The fainter dashed lines correspond to changing the propagation parameters to MIN (lower) and MAX (upper). The fainter dotted lines correspond to changing the DM profile to isothermal (lower) and Moore (upper).

uncertainty will be reduced by future measurements of cosmic rays and is, however, present only at $E \ll M_{\text{DM}}$.

5.2. Electrons + positrons

The computation of the fluxes of $e^+ + e^-$ from MDM annihilations is just a rearrangement of the calculations for positrons presented in the previous section. Figure 7 shows the predicted flux as compared to the results from the balloon experiments ATIC, PPB-BETS and EC and HESS. It is apparent that the MDM predictions are not compatible with the peak individuated (mainly) by the ATIC data points: a spectrum, which is flat up to the higher energies, with a smooth endpoint somewhat below M would be expected. The HESS datapoints indicate a steepening of the spectrum with respect to GeV energies. They are compatible with the shoulder of the ATIC peak, which however cannot be fully tested.

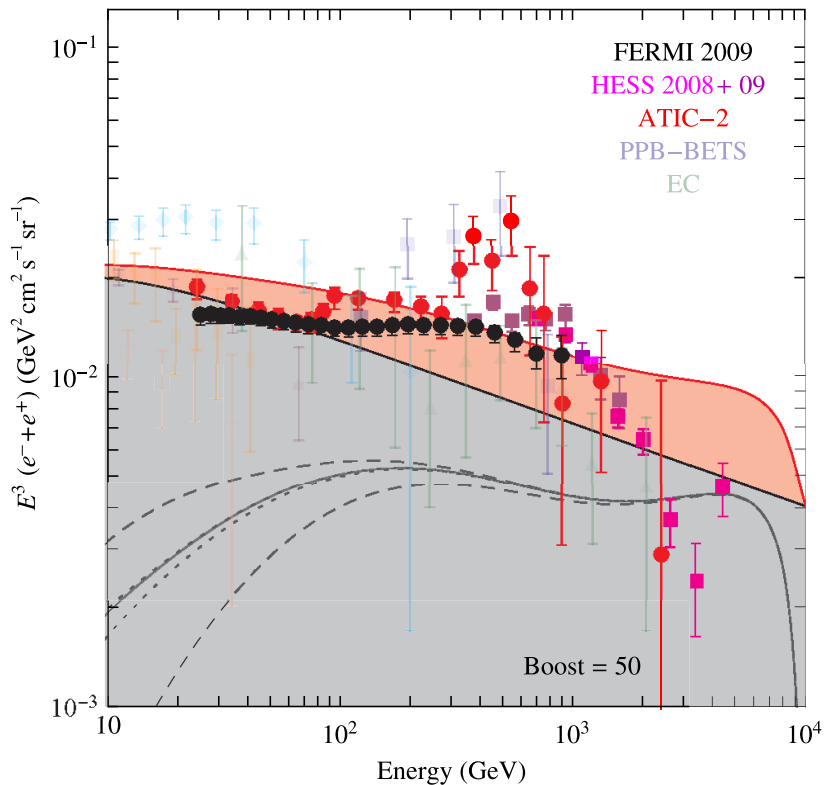


Figure 7. Sum of electrons and positrons. The flux of electrons and positrons from MDM annihilations is compared to the data from ATIC, PPB-BETS, EC and previous experiments, plus the datapoints from HESS and FERMI. The main result (solid line and shaded area) is computed assuming a benchmark NFW DM profile and MED propagation parameters. The fainter dashed lines correspond to changing the propagation parameters to MIN (lower) and MAX (upper). The fainter dotted lines correspond to changing the DM profile to isothermal (lower) and Moore (upper).

If the presence of the ATIC peak is confirmed in future data sets, therefore strongly indicating a DM mass around 1 TeV, MDM will be falsified.

Assuming that the astrophysical background is a power law (HESS data, however, indicate a steepening around 1 TeV), the MDM 5-plet predicts a slightly harder quasi-power-law $e^+ + e^-$ spectrum up to several TeV energies¹³.

¹³ *Note added.* The ATIC peak, which was incompatible with MDM, is now contradicted by the new more precise FERMI data [63] (unless an exceptionally bad energy resolution is assumed for FERMI), that we just superimposed to figure 7, without modifying the MDM prediction to better fit the new data. The problem is now that FERMI data are consistent with the steepening apparent in the HESS data (supplemented by the new results at lower energy in [64]). If this feature will be confirmed and cannot be attributed to the astrophysical background, MDM will be excluded as an interpretation of the PAMELA and FERMI e^\pm excesses.

5.3. Antiprotons

The propagation of antiprotons through the galaxy is described by a diffusion equation analogous to the one for positrons. Again, the number density of antiprotons per unit energy $f(t, \vec{x}, T) = dN_{\bar{p}}/dT$ vanishes on the surface of the cylinder at $z = \pm L$ and $r = R$. $T = E - m_p$ is the \bar{p} kinetic energy, conveniently used instead of the total energy E (a distinction that will not be particularly relevant for our purposes as we look at energies much larger than the proton mass m_p). Since $m_p \gg m_e$ we can neglect the energy loss term, and the diffusion equation for f is

$$\frac{\partial f}{\partial t} - K(T) \cdot \nabla^2 f + \frac{\partial}{\partial z} (\text{sign}(z) f V_{\text{conv}}) = Q - 2h \delta(z) \Gamma_{\text{ann}} f. \quad (24)$$

The pure diffusion term can again be written as $K(T) = K_0 \beta (p/\text{GeV})^\delta$, where $p = (T^2 + 2m_p T)^{1/2}$ and $\beta = v_p/c = (1 - m_p^2/(T + m_p)^2)^{1/2}$ are the antiproton momentum and velocity. The V_{conv} term corresponds to a convective wind, assumed to be constant and directed outward from the galactic plane, that tends to push away \bar{p} with energy $T \lesssim 10 m_p$. The different sets of values of the parameters are given in table 2. The last term in equation (24) describes the annihilations of \bar{p} on interstellar protons in the galactic plane (with a thickness of $h = 0.1 \text{ kpc} \ll L$) with rate $\Gamma_{\text{ann}} = (n_H + 4^{2/3} n_{\text{He}}) \sigma_{\text{pp}}^{\text{ann}} v_{\bar{p}}$, where $n_H \approx 1 \text{ cm}^{-3}$ is the hydrogen density, $n_{\text{He}} \approx 0.07 n_H$ is the helium density (the factor $4^{2/3}$ accounting for the different geometrical cross section in an effective way) and the $\sigma_{\text{pp}}^{\text{ann}}$ given explicitly in [5, 30, 43]. We neglect the effect of ‘tertiary antiprotons’. This refers to primary \bar{p} after they have undergone non-annihilating interactions on the matter in the galactic disc, losing part of their energy.

In the ‘no-tertiaries’ approximation that we adopt, the solution [44]–[46] for the antiproton flux at the position of the earth $\Phi_{\bar{p}}(T, \vec{r}_\odot) = v_{\bar{p}}/(4\pi) f$ acquires a simple factorized form (see e.g. [35])

$$\Phi_{\bar{p}}(T, \vec{r}_\odot) = B \frac{v_{\bar{p}}}{4\pi} \left(\frac{\rho_\odot}{M_{\text{DM}}} \right)^2 R(T) \sum_k \frac{1}{2} \langle \sigma v \rangle_k \frac{dN_{\bar{p}}^k}{dT}, \quad (25)$$

where B is the boost factor. The k index runs over all the annihilation channels with antiprotons in the final state, with the respective cross sections; this part contains the particle physics input. The function $R(T)$ encodes all the astrophysics and depends on the choice of halo profile and propagation parameter set. It is plotted in figure 5 for several possible choices. Finally, for completeness we also take into account the solar modulation effect, due to the interactions with the solar wind, that distorts the spectrum via a slight increase of the low energy tail, as described in more detail in [5, 47].

The astrophysical background is predicted by the detailed analysis in [48], the results of which we find to be well reproduced by a fitting function of the form $\log_{10} \Phi_{\bar{p}}^{\text{bkg}} = -1.64 + 0.07 \tau - \tau^2 - 0.02 \tau^3 + 0.028 \tau^4$ with $\tau = \log_{10} T/\text{GeV}$. We take for definiteness the flux corresponding to the ‘MED’ propagation parameters. Particularly favorable is the fact that the uncertainty in the estimates of the background is quite narrow around 10–100 GeV, where results are expected soon.

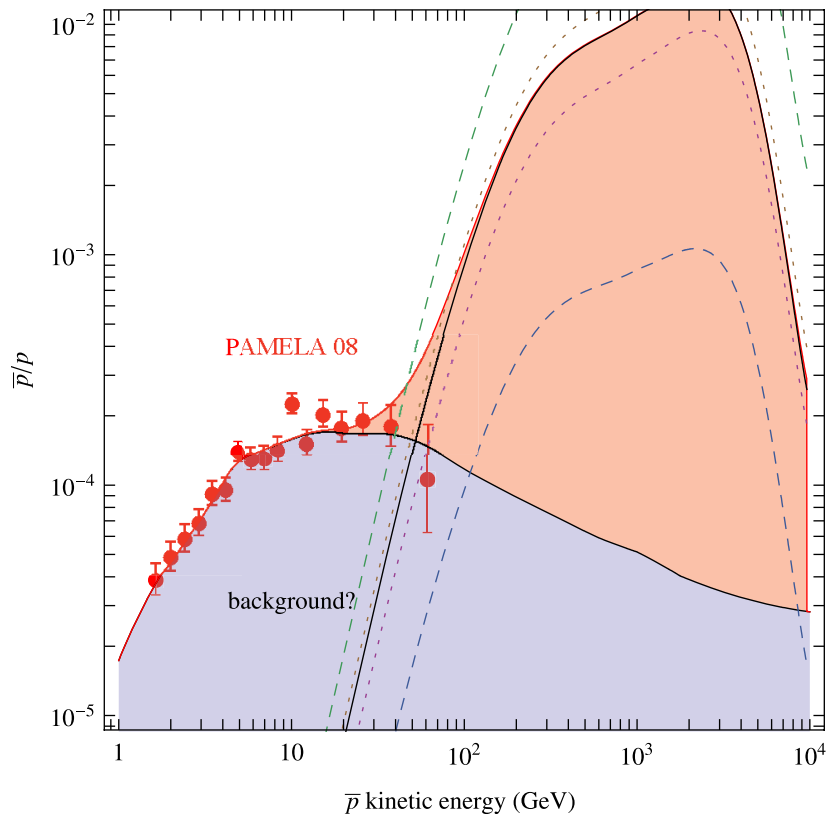


Figure 8. Antiprotons. The antiproton over proton ratio (at top of the atmosphere) from MDM annihilations, compared to the recent PAMELA data. We have assumed the same boost factor as for positrons ($B = 50$). The main result (solid line and shaded area) is computed assuming a benchmark NFW DM profile and MED propagation parameters. The fainter dashed lines correspond to changing the propagation parameters to MIN (lower) and MAX (upper). The fainter dotted lines correspond to changing the DM profile to isothermal (lower) and Moore (upper).

Figure 8 shows the results for the final \bar{p} flux from MDM annihilations at Earth (at the top of the atmosphere), normalized to the one of protons, compared to the background and to the most recent PAMELA data (older experimental data point are no longer significant). We have assumed the same boost factor as for positrons, although in principle it could be different [40]. As apparent, the agreement with the data is quite good. A prominent excess is predicted to show up at energies slightly above those that have been probed by PAMELA so far. This is a consequence of the large mass of the MDM candidate and also of the annihilation channel into W^+W^- . The figure is produced with the benchmark choices of NFW and MED. The shape of the spectrum is relatively independent from the propagation model and the halo profile. Different \bar{p} propagation models instead change the overall signal rate by about one orders of magnitude. Different halo profiles with fixed ρ_\odot make only a difference of a factor of a few, which can be interpreted in terms of the fact that the signal is not dominated by the far galactic center region, where profiles differ the most.

5.4. Gamma rays

Gamma ray signals from DM annihilation in the regions where DM is more dense can be very significant, but also depend strongly on the astrophysical assumptions, such as in particular the galactic DM profile. The spectra of high-energy γ rays from the galactic center in the Minimal DM case have been presented in [4, 5]: the spectrum is characterized by a (smeared) line at $E \approx M$ and a continuum that extends to lower energies. Most astrophysical detections of gamma ray fluxes are, however, compatible with power-law fluxes: the most conservative approach is therefore to assume that the observed fluxes are of standard (yet unknown) astrophysical origin and impose that the flux from DM does not exceed such observations. This imposes stringent constraints on the DM annihilation cross section and the DM halo profiles.

A complete, model-independent calculation has been carried out in this respect in [49], which considers bounds from high-energy gamma rays from the galactic center, the galactic ridge and the Sagittarius dwarf galaxy, but also radio waves from the galactic center (produced by synchrotron radiation in the strong magnetic field by the electrons and positrons from DM annihilations). Such bounds apply of course in particular to the case of a particle with a 9.6 TeV mass and W^+W^- main annihilation channel (figure 4 in [49]) such as MDM: it is found that the annihilation cross section in equation (19) is (marginally) allowed in the case of a NFW DM profile in the Milky Way and the Sagittarius dwarf galaxy. It has, however, to be assumed that no boost factor is present for signals from the galactic center, which is possible if DM clumps are tidally disrupted in the central regions of the Milky Way. Alternatively, perhaps more realistically, but in tension with state-of-the-art numerical simulations, choosing less steep profiles such as isothermal allows us to pass the constraints. Recent studies [50, 51] along these lines for dwarf galaxies find comparable or looser constraints.

6. Collider searches

At an accelerator like the Large Hadron Collider (LHC), which will soon (er or later) operate colliding pp at $\sqrt{s} = 14$ TeV, DM particles can in principle be pair produced, and this is a very promising way to search for DM and measure its properties.

In the case of MDM, for any multiplet with $Y = 0$ and arbitrary n the partonic total cross sections (averaged over initial colors and spins) for producing any of its component are

$$\hat{\sigma}_{u\bar{d}} = \hat{\sigma}_{d\bar{u}} = 2\hat{\sigma}_{u\bar{u}} = 2\hat{\sigma}_{d\bar{d}} = \frac{g_X g_2^4 (n^2 - 1)}{13824 \pi \hat{s}} \beta \cdot \begin{cases} \beta^2, & \text{if } \mathcal{X} \text{ is a scalar,} \\ 3 - \beta^2, & \text{if } \mathcal{X} \text{ is a fermion,} \end{cases} \quad (26)$$

where the subscripts denote the colliding partons, and $\beta = \sqrt{1 - 4M^2/\hat{s}}$ is the DM velocity with respect to the partonic center-of-mass frame. Production of non-relativistic scalars is p -wave suppressed in the usual way. It is obvious that the production of the 5-plet with $M = 9.6$ TeV is kinematically impossible. Possible upgrades of LHC luminosity and magnets are discussed in [52].

If produced in collisions, MDM has a clean signature: the small mass splitting ΔM among the DM components makes charged MDM component(s) enough long-lived that they manifest in the detector as charged tracks. Irrespectively of the DM spin the lifetime of DM^\pm particles with $Y = 0$ and $n = \{3, 5, 7, \dots\}$ is $\tau \simeq 44 \text{ cm}/(n^2 - 1)$ and the decay channels are precisely

determined as

$$\begin{aligned}
 \text{DM}^\pm &\rightarrow \text{DM}^0 \pi^\pm : \Gamma_\pi = (n^2 - 1) \frac{G_F^2 V_{ud}^2 \Delta M^3 f_\pi^2}{4\pi} \sqrt{1 - \frac{m_\pi^2}{\Delta M^2}}, & \text{BR}_\pi &= 97.7\%, \\
 \text{DM}^\pm &\rightarrow \text{DM}^0 e^\pm (\bar{\nu})_e : \Gamma_e = (n^2 - 1) \frac{G_F^2 \Delta M^5}{60\pi^3}, & \text{BR}_e &= 2.05\%, \\
 \text{DM}^\pm &\rightarrow \text{DM}^0 \mu^\pm (\bar{\nu})_\mu : \Gamma_\mu = 0.12 \Gamma_e, & \text{BR}_\mu &= 0.25\%
 \end{aligned} \tag{27}$$

having used the normalization $f_\pi = 131 \text{ MeV}^{14}$ and the ΔM of equation (14), which accidentally happens to be the value that maximizes BR_π . The DM^+ life-time is long enough that decays can happen inside the detector. On the contrary, the faster decays of $\text{DM}^{\pm\pm}$ particles (present for $n \geq 5$) mostly happen within the non-instrumented region with few cm size around the collision region. Measurements of τ and of the energy of secondary soft pions, electrons and muons constitute tests of the model, as these observables negligibly depend on the DM mass M . On the contrary, measurements of the total number of events or of the DM velocity distribution would allow us to infer its mass M and its spin. Although SM backgrounds do not fully mimic the well-defined MDM signal, at a hadron collider (such as the LHC) their rate is so high that it seems impossible to trigger on the MDM signal.

Note that extra $SU(2)_L$ multiplets that couple (almost) only through gauge interactions tend to give a LHC phenomenology similar to the one discussed above, irrespectively of their possible relevance for the MDM problem. On the contrary, DM candidates like neutralinos are often dominantly produced through gluino decays, such that DM is accompanied by energetic jets rather than by charged tracks.

7. Other phenomenological signatures

The characteristic small mass splitting ΔM between the neutral DM and the charged components of the multiplet allows for a few other interesting albeit quite speculative manifestations of MDM.

7.1. Accumulator

One could envision accelerating a large amount of protons p or nuclei \mathcal{N} in an accumulator ring and having them collide on the DM particles of the galactic halo bath, that would therefore act as a diffuse target. At energies $E_{p,\mathcal{N}} > \Delta M$ the charged current (CC) collision $\text{DM} \mathcal{N} \rightarrow \mathcal{N}^\pm \text{DM}^\mp$ becomes kinematically possible and the DM^\mp product would scatter out of the beam pipe giving a signature (collider experiments need instead a much larger energy $E_p \gtrsim M$ in order to pair produce DM). An estimate of the event rate gives

$$\frac{dN}{dt} = \varepsilon N_p \sigma \frac{\rho_{\text{DM}}}{M} = \varepsilon \frac{10}{\text{year}} \frac{N_p}{10^{20}} \frac{\rho_{\text{DM}}}{0.3 \text{ GeV cm}^{-3}} \frac{\text{TeV}}{M} \frac{\sigma}{3\sigma_0}, \tag{28}$$

where ρ_{DM} is the local DM density and ε is the detection efficiency, related e.g. to the fraction of beam that can be monitored. $\sigma_0 = G_F^2 M_W^2 / \pi = 1.1 \times 10^{-34} \text{ cm}^2$ is a reference partonic

¹⁴ For a recent review of chiral perturbation theory see [53].

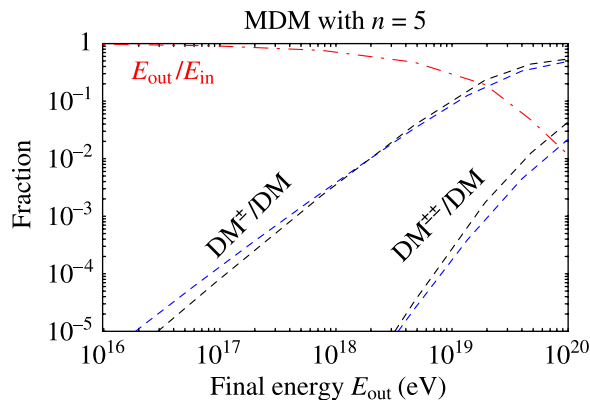


Figure 9. MDM in UHECR. The fraction of DM particles that exit from an Earth-crossing journey in the charged states DM^\pm and $DM^{\pm\pm}$ (dashed lines; the results of numerical and semi-analytical computations are represented by the paired lines that almost coincide), as a function of the exit energy E_{out} . The red dot-dashed line shows the ratio E_{out}/E_{in} and allows us to reconstruct the initial energy with which they must have entered the other side of the Earth. For instance, one reads that about 10% of the DM particles that exit the Earth at 10^{19} eV do so in the DM^\pm state; they have lost about 2/3 of their E_{in} in the journey. This fraction has to be multiplied by the flux of UHECR and by the fraction of it which is assumed to be made of MDM particles in order to get an actual event rate. UHECR have been detected up to a few 10^{20} eV.

cross section: at large energies $M_W \lesssim E_p \lesssim M$ the MDM-quark cross section approaches $3\sigma_0(n^2 - 1)/4$. Proton drivers currently planned for neutrino beam experiments can produce more than 10^{16} protons per second, and accumulating $N_p \sim 10^{20}$ protons is considered as possible, so that the number of expected events looks not unreasonable. The main problem, however, seems to be disentangling the signature from the beam-related backgrounds, such as collisions on residual gas.

7.2. Ultra high energy cosmic rays (UHECR)

If MDM particles are somehow a component of the UHECR, the already relatively long half-life of DM^\pm is Lorentz-dilated to macroscopical distances, and the possibility opens of seeing spectacular signatures in the form of km-long charged tracks of DM^\pm in detectors like IceCUBE or Antares. Consider a flux of DM^0 particles that is crossing the Earth at UHE. Via CC interactions with nucleons of Earth's matter, DM^\pm particles are produced. Being charged particles traveling in a medium, these lose a part of their energy and eventually decay back to DM^0 particles. This chain of production and decay is analogous to the process that tau neutrinos undergo in matter (ν_τ -regeneration'). In the $n = 5$ case, $DM^{\pm\pm}$ states are also produced and decay. Such a system is described by a set of coupled integro-differential equations for the evolution of the fluxes of DM^0 , of DM^\pm and of $DM^{\pm\pm}$ as a function of their energy and the position through the Earth. At high energies, the CC cross-section interactions are large (for $E \gtrsim 10^{15}$ eV DM particles interact on average at least one time along the whole diameter of the Earth), but so are also the energy losses and the Lorentz-dilated mean life of DM^\pm and $DM^{\pm\pm}$, so that a detailed analysis (numerical or semi-analytical) is necessary. The results are reported in

figure 9(b): the relevant phenomenological variable is the fraction of particles, at a given energy, that on average would emerge from their Earth crossing in the charged state and therefore would leave detectable tracks in the neutrino telescopes. One sees that, at high energies, such a fraction can be sizable. However, at those very high energies the overall flux of cosmic rays is not vanishing but fairly faint, so that the overall number of events would be limited. Moreover, it seems challenging to construct a mechanism for accelerating MDM particles at UHECR energies in the first place. They could, however, be a component of cosmic rays generated by the decay of ultra-heavy particles, in the so called ‘top-down’ scenario for the explanation of the origin of UHECR. Finally, particle identification in a detector like IceCUBE or Antares poses difficulties: DM^\pm would roughly look like muons (produced by neutrino interactions) with fake energy $E_\mu = E_\pm \beta_{CC}/\beta_\mu \sim 10^{-4} E_\pm$, because muon energy losses are approximatively given by $-dE_\mu/d\ell = \alpha + \beta_\mu E_\mu$ with $\beta_\mu \approx 0.2 \text{ kmwe}^{-1}$ [56] (β is roughly inversely proportional to the particle mass). One therefore needs to carefully study the energy loss profile along the charged tracks to see the difference between a DM^\pm with $E_\pm \sim 10^{18} \text{ eV}$ and a muon with $E_\mu \sim 10^{14} \text{ eV}$. Larger and more densely instrumented detectors seem necessary to study these issues.

8. Conclusions and outlook

As experimental searches for DM proceed more vigorously than ever, many models may finally have the chance of being tested. Supersymmetric DM, Kaluza–Klein DM, Little Higgs DM, etc all make predictions that, however (i) inscribe themselves into the context of oddly not-yet-found EW-scale New Physics; (ii) typically depend on a large number of unknown model parameters, so that DM phenomenology remains dark; (iii) usually rely on the existence of some extra feature (R-, KK-, T-parity) imposed by hand in order to be kept stable against decay into SM particles.

The MDM proposal takes on a more minimal approach: focusing on the DM problem only, we add to the SM just one extra multiplet \mathcal{X} with EW interactions (such that it does not ruin the successful predictions that the SM makes in its renormalizable limit: conservation of baryon number, lepton number, lepton flavor, etc), and investigate whether it can constitute a good DM candidate: electrically neutral, stable, produced in the right amount via the thermal freeze-out in the early Universe and not excluded by direct DM detection results. We find that indeed the construction selects one preferred candidate, the fermionic $SU(2)_L$ quintuplet with hypercharge $Y = 0$, the main phenomenological properties of which are listed in table 3. These properties are univocally computed, as no free parameters are present in the model. Also, no extra feature is introduced by hand to guarantee its stability: simply no decay modes exist consistently with the SM gauge symmetry (analogously to the stability of the proton in the SM). Phenomenological predictions can be univocally listed:

- The univocal MDM signature at **colliders** is production of DM^\pm , that manifests as a non-relativistic charged track (straight despite the magnetic field $B \sim \text{tesla}$ in the detector) that decays with a relatively long life-time of $\tau \simeq 1.8 \text{ cm}$ (due to the small splitting) into $DM^0 \pi^\pm$, leaving a quasi-relativistic curved track. However, this signature will not be visible at LHC, because the mass of the preferred MDM candidate is too large (see [52] for possible LHC upgrades) and because this signature is too complex for triggers (given their speed and the rate of QCD backgrounds).

- + The next generation of **direct detection** experiments, such as Super-CDMS or xenon 1-ton, prospect to be sensitive to the spin-independent scattering cross section of the MDM candidate on nuclei, see figure 3. MDM cannot account for the controversial annual modulation claimed by DAMA/Libra.
- + **Indirect DM searches** constitute arguably the most interesting testing ground for the MDM model. The predictions of the theory had been presented in [5] and can now be confronted to the recent experimental results from PAMELA, ATIC and HESS, of course under the assumption that these are interpreted in terms of DM annihilations. The main features of the predicted spectra are determined by the following main properties of the model:
 - the DM mass is very large (9.6 TeV), so that fluxes are expected to extend to multi-TeV energies;
 - the predominant annihilation channel is into W^+W^- channel, that produces fluxes of all species (e^+ , \bar{p} , γ and ν) with a characteristic spectrum;
 - the total annihilation cross section is very large (of the order of $10^{-23} \text{ cm}^3 \text{ s}^{-1}$) thanks to the non-perturbative Sommerfeld enhancement, which is present due to the exchange of EW gauge bosons between the annihilating particles, as reviewed in appendix A.

The profile of DM distribution in the galaxy and the propagation of the fluxes of charged antimatter in the galaxy introduce an uncertainty on the final spectra that is, however, of limited impact, essentially because the large mass of the MDM particle produces fluxes of high-energy final products that do not travel for long in the galaxy otherwise they would lose all their energy (the dependence on the propagation parameters remains more significant, at the level of one order-of-magnitude, on \bar{p} fluxes). Figures 6–8 illustrate that:

- + The MDM 5-plet prediction agrees with the **PAMELA data on the positron fraction**, if an astrophysical boost factor of $B \simeq 50$ is introduced (reduced to $B \simeq 5$ within the 3σ allowed uncertainty range for the annihilation cross section). The model predicts a continuous rise up to an energy corresponding to the DM mass of about 10 TeV.
- + The MDM 5-plet prediction agrees with the **PAMELA data on antiproton/proton fluxes**, assuming the same astrophysical boost factor. The reason of the agreement is that the excess in \bar{p} corresponding to the excess in e^+ starts at energies slightly higher than those probed by PAMELA so far. Therefore the model predicts a very relevant anomaly in future PAMELA or AMS-02 data with respect to the expected background.
- The MDM 5-plet flux of the sum of electrons and positrons is **not compatible with the peak suggested by ATIC** and PPB-BETS data at around 600 GeV: an $e^+ + e^-$ spectrum which is flat up to larger energies is expected instead. The HESS observations hint to a steepening in the $e^+ + e^-$ spectrum, without however testing the peak. New data should soon clarify the experimental situation, possibly falsifying MDM¹⁵.

¹⁵ *Note added.* The ATIC peak, incompatible with MDM predictions, is now contradicted by the new FERMI data [63] (unless an exceptionally bad energy resolution is assumed for FERMI). However, FERMI data are consistent with the steepening apparent in the HESS data (recently supplemented by the new results at lower energy in [64]).

Table 3. Main phenomenological properties of the preferred MDM candidate. Estimates of the theory uncertainties on the numerical values are given in the text.

‘Definition’	DM mass M	Splitting ΔM	Direct detection σ_{SI}	Galactic annihilation	
				$\langle\sigma v\rangle$	Channel
Fermionic $SU(2)_L$ 5-plet $Y = 0$	9.6 TeV	166 MeV	$1.2 \times 10^{-44} \text{ cm}^2$	$1.1 \times 10^{-23} \frac{\text{cm}^3}{\text{sec}}$	W^+W^-
				$3.3 \times 10^{-24} \frac{\text{cm}^3}{\text{sec}}$	ZZ
				$2.0 \times 10^{-24} \frac{\text{cm}^3}{\text{sec}}$	γZ
				$3.0 \times 10^{-25} \frac{\text{cm}^3}{\text{sec}}$	$\gamma\gamma$

- ~ The production of gamma rays (and of radio synchrotron emission from the e^\pm) from the MDM 5-plet at the galactic center and in dwarf galaxies are compatible with the observations for an NFW or Einasto profile if the astrophysical boost is assumed not to be present for observations in the gamma channel towards the galactic center, or if a not-too-steep DM profile such as isothermal is assumed (somewhat in tension with numerical simulations).
- ~ Neutrinos from the annihilations of MDM trapped at the Sun’s center are not expected to be detectable, as the fluxes depend on the inverse of the square of the DM mass (which is large) and the spin-dependent capture cross section on solar nuclei is small. Neutrinos from the galactic center can be relevant for detectors with sensitivity larger than the current one by a few orders of magnitude. Anti-deuterium fluxes are expected to be out of the reach of planned searches.

If the anomalies in the fluxes of leptons (e^+ fraction and $e^+ + e^-$) in the ranges of energies currently explored will turn out to be of astrophysical origin, e.g. from one or more local pulsars [54, 55]¹⁶, the predictions of MDM (as well as of most DM models) will be drowned in an unsuppressible background. The MDM model is peculiar in predicting, however, excesses that continue up to 10 TeV in these channels. Also, the prediction for the flux of antiprotons (much more difficult to mimic with astrophysics) would remain, and it cannot be reduced below a minimum level: with unit boost factor, the MDM flux is still marginally above the background for most choices of parameters, albeit concentrated at very high energies.

- + Constraints on the amount of energy deposited by DM annihilations at the time of BBN (when the velocity of the DM particles can be $\lesssim 10^{-3}$) impose an upper bound on the annihilation cross section. They were recently reconsidered by Hisano *et al* [57] after [58] and references therein: the annihilation cross section of MDM equation (19) is found to be allowed (see e.g. figure 2 of [57]; note that for MDM σv is already at saturation at $\beta \simeq 10^{-3}$, see figure 1(b)).

Further experimental results are expected soon.

¹⁶ See also the recent study in Hooper *et al* in [54]. See also Serpico in [54] for an agnostic analysis.

Acknowledgments

We thank our collaborators Nicolao Fornengo, Matteo Tamburini, Roberto Franceschini, Carolin Bräuninger and Paolo Panci. We thank the EU Marie Curie Research and Training network ‘UniverseNet’ (MRTN-CT-2006-035863) for support.

Appendix A. Sommerfeld effects

The DM DM annihilation cross section gets enhanced if DM particles have a non-relativistic velocity $\beta \ll 1$ and there is a long-range attractive force between them. Technically, the effect arises because annihilating DM particles cannot be approximated as plane waves, so their wavefunction must be computed by solving the Schrodinger equation in presence of the long-range potential V . For a single Abelian massless vector with potential $V = \alpha/r$ the result is $\sigma = S\sigma_{\text{perturbative}}$ where the Sommerfeld correction is [59]¹⁷

$$\mathcal{S}(x) = \frac{-\pi x}{1 - e^{\pi x}}, \quad x = \frac{\alpha}{\beta}. \quad (\text{A.1})$$

Here $\alpha < 0$ describes an attractive potential that leads to an enhancement $\mathcal{S} > 1$, and $\alpha > 0$ describes a repulsive potential that leads to $\mathcal{S} < 1$. The above results hold for the s-wave ($L = 0$) partial wave that dominates in the non-relativistic limit: the s-wave annihilation cross section $\sigma\beta$ roughly grows as $1/\beta$ for $\beta \lesssim \alpha$. Higher waves ($L > 0$) are enhanced by higher powers of α/β [61] such that, as $\beta \rightarrow 0$ all partial cross sections grow as $1/\beta$, but with negligible coefficients suppressed by α^{2L} .

The Sommerfeld enhancement is automatically present in the MDM case, since the MDM particle is coupled to the SM W, Z vectors and it is significantly heavier than them. As a consequence the s-wave annihilation cross section $\sigma\beta$ grows as $1/\beta$ for $1 \gtrsim \beta \gtrsim M_W/M \sim 10^{-3}$. This is why a possibly large positron excess had been predicted in the MDM framework before the PAMELA results¹⁸.

In the MDM framework the force vectors (the weak gauge bosons) are massive and non-Abelian: the computation of the Sommerfeld effect is more involved as one must classify the two-body DM DM states according to their conserved quantum numbers: angular momentum S , total spin L and total electric charge Q . Cirelli *et al* [4] present all the details of the calculations in the different cases. Here we focus on the DM^0DM^0 state of the 5-plet, relevant for astrophysical signals, which lies in the $Q = 0, L = 0, S = 0$ sector containing 3 states: $\{\text{DM}^{++}\text{DM}^{--}, \text{DM}^+\text{DM}^-, \text{DM}^0\text{DM}^0\}$. The ‘potential’ V and the ‘annihilation rate’ Γ become 3×3 matrices, whose off-diagonal components (and especially their signs) do not have an intuitive meaning and are defined in terms of the real and imaginary parts of the two-body

¹⁷ See also the previous work of Belotsky *et al* [59] and references therein. The relevance of non-perturbative electroweak corrections to DM freeze-out was pointed out in Hisano *et al* [59].

¹⁸ In other DM models, *ad hoc* light new particles are often introduced such that the Sommerfeld enhancement allows us to accommodate the PAMELA anomaly (as it suggests a $\sigma\beta$ at $\beta \sim 10^{-3}$, which is a few orders of magnitude larger than the $\sigma\beta \approx 310^{26} \text{ cm}^3 \text{ s}^{-1}$ at $\beta \sim 0.2$ suggested by the cosmological DM abundance).

matrix propagators. The explicit result is [4]

$$V = \begin{matrix} & \begin{matrix} -- & - & 0 \end{matrix} \\ \begin{matrix} ++ \\ + \\ 0 \end{matrix} & \begin{pmatrix} 8\Delta - 4A & -2B & 0 \\ -2B & 2\Delta - A & -3\sqrt{2}B \\ 0 & 0 & -3\sqrt{2}B \end{pmatrix} \end{matrix}, \quad \Gamma = \begin{matrix} & \begin{matrix} ++ & + & 0 \end{matrix} \\ \begin{matrix} -- \\ - \\ 0 \end{matrix} & \begin{pmatrix} 12 & 6 & 2\sqrt{2} \\ 6 & 9 & 5\sqrt{2} \\ 2\sqrt{2} & 5\sqrt{2} & 6 \end{pmatrix} \end{matrix}, \quad (A.2)$$

where $\Delta = 166 \text{ MeV}$, $A = \alpha_{\text{em}}/r + \alpha_2 c_W^2 e^{-M_{Zr}}/r$ and $B = \alpha_2 e^{-M_{Wr}}/r$. The Sommerfeld enhancement can now be computed by numerically solving the matrixial Schroedinger equation.

Co-annihilation with all other DM components enter in the computation of the cosmological freeze-out abundance, so that a lengthy computation is needed. We here discuss how one can perform a simplified computation in the limit of unbroken $SU(2)_L$, neglecting the SM vector masses $M_{W,Z}$ and the MDM intra-multiplet mass splitting Δ . This approximation is good enough for the cosmological computation. Group theory allows us to reduce the unbroken non-Abelian Sommerfeld enhancement to a combination of Abelian-like enhancements in the various sectors¹⁹, classified according to the conserved quantum numbers: L , S and iso-spin I . We can focus on s-wave annihilations ($L = 0$) and on states with $I \leq 5$, that annihilate at tree-level into two SM particles. The Pauli principle restricts the allowed states to be $(I, S) = (3, 1)$, $(1, 0)$ and $(5, 0)$. After performing the relevant thermal average, the s-wave coefficient of equation (10) gets Sommerfeld enhanced to

$$c_s = \underbrace{\frac{30g_2^4}{\pi} \mathcal{S}(-5\alpha_2\sqrt{M/T})}_{(I,S)=(1,0) \rightarrow W^a W^a} + \underbrace{\frac{105g_2^4}{2\pi} \mathcal{S}(-3\alpha_2\sqrt{M/T})}_{(I,S)=(5,0) \rightarrow W^a W^b} + \underbrace{\left(1 + \frac{1}{24}\right) \frac{45g_2^4}{\pi} \mathcal{S}(-6\alpha_2\sqrt{M/T})}_{(I,S)=(3,1) \rightarrow \Psi\Psi, HH}. \quad (A.3)$$

The resulting DM freeze-out abundance is shown in the left panel of figure 1 (dashed line), compared with the full computation (continuous line).

Appendix B. Next-to-minimal MDM

In this appendix, we briefly sketch the directions into which the model can be extended, if the request of full minimality is abandoned and some tools of DM model building (commonly used elsewhere) are introduced.

In section 2, we rejected the candidates that have dimension-4 or dimension-5 interactions with SM fields and can therefore decay into SM particles in a time much shorter than the age of the universe. By invoking some ad hoc extra symmetry that prevents the decays, these candidates can of course be reallowed. This is actually also what happens in the case of the best know WIMP DM candidates: in SUSY models, by assigning odd R -parity to the supersymmetric partners including the LSP DM, the decay operators, that feature just one DM state, are forbidden. An equivalent mechanism is used in little-Higgs models (T -parity), in ‘universal’ extra dimension models (KK-parity), etc. Some of the MDM candidates that are rescued by the imposition of the extra symmetry resemble to particles that appear in a variety of other contexts: e.g. scalar triplets in little-Higgs models; fermion or scalar triplet in see-saw

¹⁹ For a generic unbroken non-Abelian gauge interaction, the group theory needed to compute the Sommerfeld effect was presented in [60].

models; KK excitations of lepton doublets or of Higgses in extra dimensional models; higgsinos, sneutrinos, winos in supersymmetric models. In general, however, these models possess a plethora of other parameters so that typically their DM candidates behave very differently from the MDM candidates. But in some corner of the parameter space the phenomenological features can coincide. The signatures of some of these candidates (in particular the ‘wino-like’ fermionic triplet and the scalar triplet) have been studied in [4, 5].

Speaking of decays, we note that the main MDM candidate (the fermion 5-plet, cosmologically stable in the minimal construction) acquires a non-negligible decay mode if Λ is somewhat below the Planck scale. The effective dimension-6 operator that dominantly contributes to the decay is $\mathcal{X}LHHH^*/\Lambda^2$. It induces 4-body decays, such as $DM^0 \rightarrow \ell^\mp W_L^\pm Z_L Z_L$ (where L denotes longitudinal polarization), with rate $\Gamma \sim M^5/4\pi\Lambda^4$. Such decays can provide an alternative interpretation of the PAMELA excess: $\Lambda \approx 10^{16}$ GeV gives a lifetime of about 10^{25} s. 2-body decays, such as $DM^0 \rightarrow \ell^\pm W^\mp$ have a rate $\Gamma_2 \sim v^4 M/(4\pi)^5 \Lambda^4$, which is subdominant as long as $M \gg 4\pi v$.

As discussed in section 4, MDM candidates with $Y \neq 0$ have an elastic cross section, which is 2–3 orders of magnitude above present direct detection bounds [9] due to the exchange of a Z boson and have therefore been rejected. A possible way to reinclude them is to abandon minimality by introducing another state that mixes with the DM: this has the effect of splitting the components of the Dirac DM particle by an amount δm such that the lightest one becomes a Majorana fermion, which cannot have a vector-like coupling to the Z boson. This is actually what happens in the well-known case of SUSY higgsino DM, via the mixing with Majorana gauginos. In our case, if a δm larger than the DM kinetic energy and smaller than $M_Q - M_0$ is generated, the only consequence would be to suppress the direct detection DM signals and the rest of the phenomenology would be essentially unchanged.

In the case of scalar DM, additional operators not listed in equation (1) are generically present: 4-scalar interactions of \mathcal{X} with Higgses and \mathcal{X} quartic self-interactions:

$$\mathcal{L} \supset -c \lambda_H (\mathcal{X}^* T_R^a \mathcal{X}) (H^* T_H^a H) - c \lambda'_H |\mathcal{X}|^2 |H|^2 - \frac{\lambda_\mathcal{X}}{2} (\mathcal{X}^* T_R^a \mathcal{X})^2 - \frac{\lambda'_\mathcal{X}}{2} |\mathcal{X}|^4, \quad (\text{B.1})$$

where T_R^a are $SU(2)_L$ generators in the representation to which R belongs and $c = 1(1/2)$ for a complex (real) scalar. In the strictly minimal theory, these terms have been assumed vanishing, as they introduce the new unknown couplings λ_H , λ'_H , $\lambda_\mathcal{X}$ and $\lambda'_\mathcal{X}$. But if minimality is relaxed they can be introduced and they allow us to enlarge the parameter space of the theory. These extra interactions do not induce DM decay (because two \mathcal{X} are involved, and we assume $\langle \mathcal{X} \rangle = 0$). They affect instead the computations of the mass splitting, of the direct detection inelastic cross section and of the relic density (therefore the determination of the DM mass). Indeed, the coupling λ_H splits the masses of the components of \mathcal{X} by an amount

$$\Delta M = \frac{\lambda_H v^2 |\Delta T_\mathcal{X}^3|}{4M} = \lambda_H \cdot 7.6 \text{ GeV} \frac{\text{TeV}}{M} \quad (\text{B.2})$$

having inserted $\langle H \rangle = (v, 0)$ with $v = 174$ GeV and $\Delta T_\mathcal{X}^3 = 1$. This cannot be neglected with respect to the splitting which is separately generated by loop corrections (discussed in section 3.1) as soon as $\lambda_H \approx 0.01$. Also, λ_H and λ'_H open the possibility of extra annihilations into Higgses

$$\langle \sigma_A v \rangle_{\text{extra}} = \frac{|\lambda_H|^2 + (n^2 - 1)|\lambda'_H|^2/16}{16\pi M^2 g_\mathcal{X}} \quad (\text{B.3})$$

(no interference terms are present). The contribution from λ_H is relevant for $\lambda_H \approx 0.01$, the same value that also produce a non-negligible mass splitting. The contribution from λ'_H is relevant for $|\lambda'_H| \sim g_Y^2, g_2^2$ or larger. In these regimes, to compute how much the inferred value of M would be affected one simply adds the contribution in equation (B.3) to those in equation (6): in general, the increase of the total annihilation cross section implies the increase of the inferred MDM mass, and the mass of the low n candidates are more affected than the high n ones, because the gauge-mediated annihilation cross sections are relatively less important for the formers. For example, a large $\lambda'_H = 1$ would increase the predicted value of M by a factor 2.4 for $n = 2$, by 20% for $n = 3$, by 2% for $n = 5$ and by 0.5% for $n = 7$. Note that $\lambda_H \sim g_2^2$ and $\lambda'_H \sim g_Y^2$ are the values predicted by some solutions to the hierarchy problem, such as SUSY and gauge/Higgs unification. Finally, nonzero couplings λ_H and λ'_H can also produce an elastic cross section σ_{SI} on nuclei, much larger than the one in equation (4), as an UV-divergent effect that corresponds to a renormalization of $|\mathcal{X}|^2|H|^2$ operators is generated.

We note that when \mathcal{X} is a neutral scalar singlet, the non-minimal annihilations in equation (B.1) are the only existing ones. In this case, the observed amount of DM is obtained for $M \approx 2.2 \text{ TeV} |\lambda'_H|$ (we are assuming $M \gg M_Z$; for generic values of M the correlation between M and λ'_H was studied in [62] and references therein).

Finally, one can envision a scenario in which more than one MDM multiplet is present at the same time. Or also a scenario in which several distinct copies ('flavors', in analogy with the SM families) of the same MDM multiplet exist. In both cases, to a good approximation their abundances evolve independently, such that the observed DM abundance is reproduced for lower values of the respective DM masses. In this more general situation, the M values in table 1 must be reinterpreted as upper bounds on M . This might bring some of the candidates within reach of the LHC.

References

- [1] Bertone G, Hooper D and Silk J 2005 *Phys. Rep.* **405** 279 (arXiv:hep-ph/0404175)
Einasto J 2009 arXiv:0901.0632
- [2] Giusti L, Romanino A and Strumia A 1999 *Nucl. Phys. B* **550** 3 (arXiv:hep-ph/9811386)
Barbieri R and Strumia A 1999 *Phys. Lett. B* **462** 144 (arXiv:hep-ph/9905281)
- [3] Cirelli M, Fornengo N and Strumia A 2006 *Nucl. Phys. B* **753** 178 (arXiv:hep-ph/0512090)
- [4] Cirelli M, Strumia A and Tamburini M 2007 *Nucl. Phys. B* **787** 152 (arXiv:0706.4071)
- [5] Cirelli M, Franceschini R and Strumia A 2008 *Nucl. Phys. B* **800** 204 (arXiv:0802.3378)
- [6] Cirelli M and Strumia A 2008 arXiv:0808.3867
- [7] Starkman G D, Gould A, Esmailzadeh R and Dimopoulos S 1990 *Phys. Rev. D* **41** 3594
Mack G D, Beacom J F and Bertone G 2007 arXiv:0705.4298
- [8] Goodman M W and Witten E 1985 *Phys. Rev. D* **31** 3059
- [9] Ahmed Z *et al* (CDMS Collaboration) 2009 *Phys. Rev. Lett.* **102** 011301 (arXiv:0802.3530)
- [10] Angle J *et al* (XENON Collaboration) 2008 *Phys. Rev. Lett.* **100** 021303 (arXiv:0706.0039)
- [11] Spergel D N *et al* (WMAP Collaboration) 2006 arXiv:astro-ph/0603449
Cirelli M and Strumia A 2006 *J. Cosmol astropart. Phys.* **JCAP12(2006)013** (astro-ph/0607086)
Tegmark M *et al* 2006 *Phys. Rev. D* **74** 123507 (arXiv:astro-ph/0608632)
- [12] Coulomb C A 1785 'Premier Mémoire sur l'Électricité et le Magnétisme' *Mém. Acad. R. Sci.* **88** 569
- [13] Bernabei R *et al* (DAMA Collaboration) 2008 *Eur. Phys. J. C* **56** 333 (arXiv:0804.2741)
- [14] Drees M and Nojiri M 1993 *Phys. Rev. D* **48** 3483

- [15] Engel J, Pittel S and Vogel P 1992 *Int. J. Mod. Phys. E* **1** 1
- [16] Aprile E and Baudis L (XENON Collaboration) 2009 *Proc. Identification of Dark Matter 2008 Conf. (Stockholm, Sweden, 18–22 Aug. 2008)* (Trieste, Italy: Proceedings of Science) pp 1–10 (arXiv:0902.4253 [astro-ph.IM])
CDMS-II Collaboration 2005 eConf C041213 (2004) 2529 (arXiv:astro-ph/0503583)
- [17] Adriani O *et al* (PAMELA Collaboration) 2008 arXiv:0810.4995
- [18] Barwick S W *et al* (HEAT Collaboration) 1997 *Astrophys. J.* **482** L191 (arXiv:astro-ph/9703192)
- [19] Aguilar M *et al* (AMS-01 Collaboration) 2007 *Phys. Lett. B* **646** 145–54 (arXiv:astro-ph/0703154)
- [20] Adriani O *et al* 2008 arXiv:0810.4994
- [21] ATIC Collaboration 2008 *Nature* **456** 362
- [22] PPB-BETS Collaboration 2008 arXiv:0809.0760 <http://ppb.nipr.ac.jp>
- [23] Aharonian F *et al* (HESS Collaboration) 2008 *Phys. Rev. Lett.* **101** 261104 (arXiv:0811.3894)
- [24] Wefel J P 2008 *Proc. IS CRA 2008 (Erice, Italy, 2008)* <http://laspace.lsu.edu/IS CRA/IS CRA2008>
- [25] Kobayashi T, Nishimura J, Komori Y, Shirai T, Tateyama N, Taira T, Yoshida K and Yuda T (EC collaboration) 1999 *Proc. 26th Int. Cosmic Ray Conf. (Salt Lake City, 1999)* vol 3 pp 61–4
- [26] FERMI Collaboration 2007 Measuring 10–1000 GeV cosmic ray electrons with GLAST/LAT Talk at the *ICRC07 conf.*
- [27] Cirelli M, Kadastik M, Raidal M and Strumia A 2008 arXiv:0809.2409
- [28] Ginzburg V L, Khazan Ya M and Ptuskin V S 1980 *Astrophys. Space Sci.* **68** 295–314
Webber W R, Lee M A and Gupta M 1992 *Astrophys. J.* **390** 96–104
- [29] Delahaye T, Lineros R, Donato F, Fornengo N and Salati P 2008 *Phys. Rev. D* **77** 063527 (arXiv:0712.2312)
- [30] Hisano J, Matsumoto S, Saito O and Senami M 2006 *Phys. Rev. D* **73** 055004 (arXiv:hep-ph/0511118)
- [31] Bahcall J N and Soneira R M 1980 *Astrophys. J. Suppl.* **44** 73
- [32] Graham A W, Merritt D, Moore B, Diemand J and Terzic B 2006 *Astron. J.* **132** 2685 (arXiv:astro-ph/0509417)
Navarro J F *et al* 2008 arXiv:0810.1522
- [33] Navarro J, Frenk C and White S 1997 *Astrophys. J.* **490** 493 (arXiv:astro-ph/9611107)
- [34] Diemand J, Moore B and Stadel J 2004 *Mon. Not. R. Astron. Soc.* **353** 624 (arXiv:astro-ph/0402267)
- [35] Donato F, Fornengo N, Maurin D and Salati P 2004 *Phys. Rev. D* **69** 063501 (arXiv:astro-ph/0306207)
- [36] Moskalenko I V and Strong A W 1998 *Astrophys. J.* **493** 694 (arXiv:astro-ph/9710124)
- [37] Baltz E A and Edsjo J 1999 *Phys. Rev. D* **59** 023511 (arXiv:astro-ph/9808243)
- [38] Delahaye T, Donato F, Fornengo N, Lavalley J, Lineros R, Salati P and Taillet R 2008 arXiv:0809.5268
- [39] Lavalley J, Pochon J, Salati P and Taillet R 2006 (arXiv:astro-ph/0603796)
- [40] Lavalley J, Yuan Q, Maurin D and Bi X J 2007 arXiv:0709.3634
- [41] Brun P, Bertone G, Lavalley J, Salati P and Taillet R 2007 *Phys. Rev. D* **76** 083506 (arXiv:0704.2543)
Bringmann T, Lavalley J and Salati P 2009 arXiv:0902.3665
- [42] Berezhinsky V, Dokuchaev V and Eroshenko Y 2003 *Phys. Rev. D* **68** 103003 (arXiv:astro-ph/0301551)
- [43] Tan L C and Ng L K 1983 *J. Phys. G: Nucl. Phys* **9** 227
- [44] Chardonnet P, Mignola G, Salati P and Taillet R 1996 *Phys. Lett. B* **384** 161 (arXiv:astro-ph/9606174)
Bottino A, Donato F, Fornengo N and Salati P 1998 *Phys. Rev. D* **58** 123503 (arXiv:astro-ph/9804137)
Bergstrom L, Edsjo J and Ullio P 1999 *Astrophys. J.* **526** 215 (arXiv:astro-ph/9902012)
- [45] Maurin D, Taillet R, Donato F, Salati P, Barrau A and Boudoul G 2002 arXiv:astro-ph/0212111
- [46] Maurin D, Donato F, Taillet R and Salati P 2001 *Astrophys. J.* **555** 585 (arXiv:astro-ph/0101231)
- [47] Gleeson L J and Axford W I 1967 *Astrophys. J.* **149** L115
Gleeson L J and Axford W I 1968 *Astrophys. J.* **154** 1011
- [48] Bringmann T and Salati P 2007 *Phys. Rev. D* **75** 083006 (arXiv:astro-ph/0612514)
- [49] Bertone G, Cirelli M, Strumia A and Taoso M 2008 arXiv:0811.3744
- [50] Pieri L, Lattanzi M and Silk J 2009 arXiv:0902.4330
- [51] Essig R, Sehgal N and Strigari L 2009 arXiv:0902.4750

- [52] Azuelos G *et al* (Atlas Collaboration) 2002 *J. Phys. G: Nucl. Phys.* **28** 2453
de Roeck A 2003 Talk at the 2003 *Int. Workshop on Future Hadron Colliders* <http://conferences.fnal.gov/hadroncollider>
Denegri D 2005 Talk at the 2005 *Les Houches Workshop* <http://lappweb.in2p3.fr/conferences/LesHouches>
- [53] Colangelo G and Isidori G 2001 arXiv:hep-ph/0101264
- [54] Atoian A M, Aharonian F A and Volk H J 1995 *Phys. Rev. D* **52** 3265
Büshing I *et al* 2008 arXiv:0804.0220
Kobayashi T, Komori Y, Yoshida K and Nishimura J 2004 *Astrophys. J.* **601** 340 arXiv:astro-ph/0308470
Hooper D, Blasi P and Serpico P D 2008 arXiv:0810.1527
Yuksel H, Kistler M D and Stanev T 2008 arXiv:0810.2784
Profumo S 2008 arXiv:0812.4457
Serpico P D 2008 arXiv:0810.4846
- [55] Piran T *et al* 2009 arXiv:0902.0376
- [56] AMSler C *et al* (Particle Data Group) 2008 *Phys. Lett. B* **667** 1
- [57] Hisano J, Kawasaki M, Kohri K, Moroi T and Nakayama K 2009 arXiv:0901.3582
- [58] Jedamzik K 2004 *Phys. Rev. D* **70** 063524 (arXiv:astro-ph/0402344)
Jedamzik K 2004 *Phys. Rev. D* **70** 083510 (arXiv:astro-ph/0405583)
Iocco F, Mangano G, Miele G, Pisanti O and Serpico P D 2008 arXiv:0809.0631
- [59] Sommerfeld A 1931 'Über die Beugung und Bremsung der Elektronen' *Ann. Phys.* **403** 257
Hisano J, Matsumoto S and Nojiri M M 2004 *Phys. Rev. Lett.* **92** 031303 (arXiv:hep-ph/0307216)
Hisano J, Matsumoto S, Nojiri M M and Saito O 2005 *Phys. Rev. D* **71** 063528 (arXiv:hep-ph/0412403)
Belotsky K, Fargion D, Khlopov M and Konoplich R V 2008 *Phys. Atom. Nucl.* **71** 147 (arXiv:hep-ph/0411093)
Hisano J, Matsumoto S, Nagai M, Saito O and Senami M 2007 *Phys. Lett. B* **646** 34 (arXiv:hep-ph/0610249)
- [60] Strumia A 2009 *Nucl. Phys. B* **809** 308 (arXiv:0806.1630)
- [61] Iengo R 2009 arXiv:0902.0688
Iengo R 2009 arXiv:0903.0317
Cassel S, Ghilencea D M and Ross G G 2009 arXiv:0903.1118
- [62] Silveira V and Zee A 1985 *Phys. Lett. B* **161** 136
McDonald J 1994 *Phys. Rev. D* **50** 3637 (arXiv:hep-ph/0702143)
Burgess C P, Pospelov M and ter Veldhuis T 2001 *Nucl. Phys. B* **619** 709 (arXiv:hep-ph/0011335)
- [63] FERMI/LAT Collaboration 2009 arXiv:0905.0025
- [64] HESS Collaboration 2009 arXiv:0905.0105